Astron. Astrophys. 331, 121–146 (1998)

ASTRONOMY
AND
ASTROPHYSICS

Chondrule formation by lightning in the Protosolar Nebula?

W. Pilipp[1], **T.W. Hartquist**[2], **G.E. Morfill**[3], **and E.H. Levy**[4]

[1] Max-Planck-Institut für Extraterrestrische Physik, D-85740 Garching, Germany (e-mail: wgp@mpe-garching.mpg.de)
[2] Max-Planck-Institut für Extraterrestrische Physik, D-85740 Garching, Germany (e-mail: twh@ipp-garching.mpg.de)
[3] Max-Planck-Institut für Extraterrestrische Physik, D-85740 Garching, Germany (e-mail: gem@mpe-garching.mpg.de)
[4] Lunar and Planetary Laboratory, University of Arizona, Tucson, Arizona 85721, USA (e-mail: ehlevy@ccit.arizona.edu)

Received 15 November 1996 / Accepted 14 July 1997

Abstract. We present results for the electric fields generated in steady one dimensional flows in media having properties that obtained in the protosolar nebula. The mean neutral velocity was taken to be constant and antiparallel to an effective gravitational field, whereas the mean gas phase ion and electron velocities as well as the velocities of entrained 0.01 cm to 1 cm radius grains and submicron- to micron-radius grains were calculated. The gas phase ionization structure was followed as were the charges carried by the grains. Grains were taken to be charged in collisions with gas phase ions and electrons; grain-grain charge transfer due to the Elster-Geitel mechanism as well as to an unspecified additional process at a parameterized rate was included.

Electric fields of sufficient strength to induce discharges, in which chondrule formation has previously been supposed to occur, were found to obtain only if the gas phase ionization rate in the nebula was almost as low as that resulting from the decay of ^{40}K and a grain-grain charge transfer mechanism in addition to the Elster-Geitel process operated. We conclude that the existence of lightning in the protosolar nebula has to depend on the operation of unknown grain-grain charge transfer processes whereas the Elster-Geitel mechanism has proved to be completely inadequate for producing lightning there. For all but a small range of model parameters the attainment of breakdown electric field strengths requires that local ionization equilibrium has not been reached. In addition, it was found that breakdown electric field strengths were more likely to be generated if the grains had an average specific mass density not much lower than of order unity.

Bearing in mind these severe constraints, we conclude that nebular lightning is possible, but requires special conditions. From considerations of the global energetics, the time scales for establishing the high field strengths plus the volume affected by discharges, we conclude that if these conditions exist lightning may have heated a large fraction of the protosolar nebula at one time or another to temperatures high enough to induce the melting of solid material.

Send offprint requests to: W. Pilipp

Key words: meteors – solar system: formation – solar system: general – dust

1. Introduction

Chondrules, a type of meteoritic inclusion, are small ($\approx 10^{-2}$g) beads of glassy rock having structures that imply that they cooled from temperatures of 1700 K on timescales of tens of minutes to hours (Fujii & Miyamoto 1983; Hewins 1983). (For a review of models proposed for chondrule formation and an evaluation of these models see Grossman, 1988; Levy, 1988). The various flash heating mechanisms that have been invoked to account for chondrule structures include: impacts (Wasson 1972; Kieffer 1975); aerodynamic drag on dust accreting onto the protosolar nebula (Wood 1984; Hood & Horanyi 1991, 1993; Ruzmaikina & Ip 1994); dissipation of shear in the nebula (Wood 1986); magnetic flares (Sonett 1979, Levy & Araki 1989); absorption of pulsed radiation of unspecified origin (Eisenhour & Buseck 1995); absorption of solar radiation as material is dragged out of the disk by a magneto-centrifugally driven wind and before it falls back to the disk (Shu et al. 1996).

The possibility that lightning occurred in the protosolar nebula and was the source of chondrule heating has also been considered (Whipple 1966; Cameron 1966; Levy 1988; Morfill & Sterzik 1990; Pilipp et al. 1992; Morfill et al. 1993; Horanyi et al. 1995; Love et al. 1995). However, the only detailed calculations of the electric field for relevant gas and dust grain number densities and specified fluid dynamics and gas phase charge and grain charge conditions were restricted to small amplitude acoustic waves (Pilipp et al. 1992). The volume associated with an acoustic wave having an electric field strong enough to trigger discharge was found to be too small to contain sufficient energy to ionize a discharge channel. According to estimates by Pilipp et al. lightning in the protosolar nebula could give rise to significant heating and ionization in the discharge channels only if it were generated on a more global scale, i.e. if the spatial extent

of a region in which the electric field is strong enough to induce discharges is larger than $10^{10}\mathrm{cm}\ \left(n_\mathrm{n}/\left(10^{14}\,\mathrm{cm}^{-3}\right)\right)^{-3/2}$ where n_n is the number density of neutral molecules of the H_2 gas. Morfill & Sterzik (1990) and Morfill et al. (1993) have suggested that global electric fields of sufficient strengths could have been established by gravitational sedimentation of dust particles and size sorting due to gas drag on these particles.

Gibbard et al. (1997) have recently performed detailed calculations for the growth and charging of dust grains (i.e. ice particles) due to collisions between the grains in the presence of turbulent gas motion in the chondrule - formation region of the protoplanetary nebula. The electrical conductivity of the nebula was estimated self-consistently under the assumption that radioactive decay of ^{40}K induced ionization in the gas. In their model grain - grain collisions give rise to the growth of grains up to a maximum size limited by assumption to 2.5 mm, and most of the mass ends up in mm - sized grains with the mass in smaller sized grains being small. Gas phase ions and electrons are removed mainly in collisions with mm - sized grains. The grain - grain charge transfer rate was calculated from a formula based on experimental results and the time scale for the evolution of the electric field is determined by the currents due to movements of charged grains as they descend under the force of gravity and by the currents of gas phase ions and electrons driven by the electric field. Whereas a similar model applied to terrestrial thunderstorm conditions results in the prediction of the growth of the terrestrial electric field to its breakdown value for lightning discharge on a realistic time scale, the model indicates that precipitation - induced lightning cannot occur in the protosolar nebula.

Gibbard et al. construct a self-consistent model, incorporating particle growth by grain-grain collisions in turbulent gas. The resulting particle-size spectrum turns out to be deficient in small grains as compared with what is observed in chondritic meteorites, where the mass of fine-grained matrix is at most a factor of a few smaller than the mass of the chondrules themselves (Scott et al. 1988). The origin of this discrepancy is not clear. On the one hand, the actual coagulation process in the nebula may have left behind a large quantity of fine-grained material for reasons not captured in the coagulation model, or collisionally induced fracturing may have returned a large quantity of fine particles to the mix. On the other hand, it may be that meteorite-matrix material had indeed been coagulated into larger — perhaps chondrule sized — accumulations before being incorporated into the meteorite parents, in agreement with the coagulation-model results, and simply avoided being melted in a chondrule-producing heating event. In any case, the particle-size distribution is a matter of some significance inasmuch as it is collisions between large and small particles that produces electric charge separation, and it is collisions on grains – mainly the smallest grains, which present the greatest surface area per unit mass – that removes free electrons and ions from the gas. Thus a larger abundance of small grains produces conditions more favorable for the production of strong electric fields.

In this paper we explore the possibility that lightning occurred in the protosolar nebula on the assumption that in many cases (but not all) the micron and/or submicron sized particles contained about half or a fifth of the solid mass. In addition, for the grain - grain charge transfer rate we do not use an expression based on experimental results as did Gibbard et al. Instead we adopt an expression showing clearly the relative importance of the Elster-Geitel mechanism (a particular charge transfer process occurring when the grains' surface charge distributions are polarized by a large scale electric field) and non-inductive charge transfer (e.g. that due to different work functions for the material of the colliding grains). The amount of charge transferred per collision by the non-inductive process depends on two free parameters. In addition, we assume in many cases that cosmic ray induced ionization was negligible and take the decay of ^{40}K as the only other source of ionization.

We present the results of calculations for the spatial dependence of the steady electric field arising in a medium with gas and dust number densities that may have obtained in the protosolar nebula at positions between Earth and Jupiter and experiencing largescale neutral gas motions antiparallel to an effective gravitational field.

Three sets of models were considered. One set is appropriate for steady convective flow perpendicular to the disk midplane at roughly the Earth's present orbit while another set is applicable to such flow at roughly Jupiter's present orbit. A third set of models is for radial flows in a subdisk with a dust - to - gas mass ratio that is enhanced by a factor of 100 over that of a typical interstellar cloud which we adopted for the other models; in such a subdisk the grains are subject (in the frame corotating with the neutral gas) to a radially inwardly directed effective gravity comparable to the radial component of the gradient of the gas thermal pressure divided by the gas mass density. Ideally, we would like to construct multidimensional time-dependent models of the electric field evolution; however, in order to maintain computational simplicity we have restricted ourselves to one independent variable which we have taken to be a spatial variable (rather than time as it would be in a one point calculation) because, as mentioned above, the spatial extent of the region in which the electric field is strong enough to induce discharge determines whether a discharge channel is heated significantly.

Each model is a five-fluid model with the fluids consisting of neutrals (the dynamics of which are specified), gas phase ions, gas phase electrons, "big" grains identical to one another with each carrying the mean charge of a big grain, and "small" grains identical to one another except for the charge carried; the small grains are divided into subfluids in which each grain carries the same charge so that the charge distribution on the small grains could be calculated. While big grain - small grain collisions are assumed to transfer charge we have assumed that no coagulation or fracturing of grains occurs. The gas phase and grain charge conditions were calculated along with the largescale electric field and fluid densities and velocities in a self-consistent manner for various assumed gas phase ionization rates and grain charging rates.

In Sect. 2 we give the fluid and electrostatic equations on which the model is based. A consideration of the rates at which momentum transfer and charge transfer between species occurs is presented in Sect. 3. Sect. 4 contains numerical results of our model calculations. In Sect. 5 we discuss results, and in Sect. 6 we give conclusions on whether lightning may have been the source of chondrule heating.

2. Model equations

The medium is described as consisting of five fluids corresponding to neutral gas particles (H_2), gaseous ions carrying one positive charge (Mg^+ ions as considered by Pilipp et al., 1992), electrons, "big" grains (all of which are assumed to be spherical and identical to one another), and "small" grains (all of which are assumed to be spherical and identical to one another except for their charges). The subscripts n, i, e, b, and s are used to signify that a given parameter refers to the respective fluid. Each big grain is assumed to carry a charge q_b equal to the average charge carried by a big grain, and $Z_\mathrm{b} \equiv q_\mathrm{b}/e$ where e is the elementary charge. The magnitude of the average charge carried by a small grain may be sufficiently small that statistical fluctuations make the assumption that each small grain carries the same charge a poor one; hence, we consider the possibility that small grains carry different charges and divide the small grain fluid into subfluids. A quantity referring to the small grain subfluid consisting of those small grains that each carry *k* elementary charges is identified with the double subscripts s and *k*.

The effective gravitational field is taken to be in the $-\hat{z}$ direction and to be $g\hat{z}$ with $g < 0$. The velocity of the *j*th fluid is, by assumption, in the $\hat{z}$ direction and is written as $v_j\hat{z}$ where v_j is always positive for $j \neq \mathrm{e}$ and can be negative for $j = \mathrm{e}$ for large electric fields. The mass density and number density of the *j*th fluid are ρ_j and n_j. $m_j \equiv \rho_j/n_j$ is constant for each fluid.

v_n is taken to be a constant, as is ρ_n. Steady flow is considered. The continuity equations for the ions and electrons are

$$\frac{\mathrm{d}}{\mathrm{d}z}(n_\mathrm{i}\, v_\mathrm{i}) = \zeta\, n_\mathrm{n} - \Gamma_\mathrm{ib}\, n_\mathrm{i}\, n_\mathrm{b} - \sum_k \Gamma_{\mathrm{i}sk}\, n_\mathrm{i}\, n_{sk} \tag{1}$$

and

$$\frac{\mathrm{d}}{\mathrm{d}z}(n_\mathrm{e}\, v_\mathrm{e}) = \zeta\, n_\mathrm{n} + \Gamma_\mathrm{eb}\, n_\mathrm{e}\, n_\mathrm{b} + \sum_k \Gamma_{\mathrm{e}sk}\, n_\mathrm{e}\, n_{sk} \tag{2a}$$

ζ is the rate per neutral particle at which radioactive decays and penetrating cosmic rays induce ionization. Γ_{jm} is the rate coefficient for species *j* to transfer an elementary charge to species *m*. The Γ_{jm}'s are considered in the next section. The neglect of ion-electron recombination relative to ion-grain and electron-grain charge transfer is justified for the protosolar nebular regions in which lightning might have occurred.

For most cases considered in the present paper a strong electric field in the positive z-direction arises leading to a bulk motion of electrons in the negative z-direction, i.e. to $v_\mathrm{e} < 0$. Then the integration of Eq. (2a) along the positive z-direction was found to be unstable. For these cases (i.e. cases presented in Figs. 1, 3, 4a, 5, and 6, except for the curves in Fig. 1 marked EG_0, EG_+, and $(\mathrm{EG}_0)_{S_\mathrm{se}=0.3}$) we use the approximation

$$0 \approx \zeta\, n_\mathrm{n} + \Gamma_\mathrm{eb}\, n_\mathrm{e}\, n_\mathrm{b} + \sum_k \Gamma_{\mathrm{e}sk}\, n_\mathrm{e}\, n_{sk} \tag{2b}$$

in place of (2a). Approximation (2b) should be correct if in Eq. (2a) the term $(\mathrm{d}/\mathrm{d}z)(n_\mathrm{e}\, v_\mathrm{e})$ is negligible compared to the term $\Gamma_\mathrm{eb}\, n_\mathrm{e}\, n_\mathrm{b} + \sum_k \Gamma_{\mathrm{e}sk}\, n_\mathrm{e}\, n_{sk}$, i.e. if the scale length for global variations along the z-direction divided by the magnitude of the electron bulk velocity is large compared to the collision time of electrons with respect to their collisions with dust particles removing the electrons from the gas phase. As may be found from estimates of corresponding electron collision times τ_e as given by (A11) and (A12) in Appendix A, together with estimates of electron bulk velocities v_e for relevant electric field strengths and from global scale lengths arising from our numerical results, relation (2b) should be a good approximation.

The continuity equation for the small grains carrying *k* elementary charges is

$$\begin{aligned}\frac{\mathrm{d}}{\mathrm{d}z}(n_{sk}\, v_{sk}) \;=\; & \sum_{k'} \nu_{k'k}\, n_{sk'} - \sum_{k'} \nu_{kk'}\, n_{sk} \\ & + \Gamma_{\mathrm{i}s(k-1)}\, n_{s(k-1)}\, n_\mathrm{i} - \Gamma_{\mathrm{e}s(k+1)}\, n_{s(k+1)}\, n_\mathrm{e} \\ & - (\Gamma_{\mathrm{i}sk}\, n_\mathrm{i} - \Gamma_{\mathrm{e}sk}\, n_\mathrm{e})\, n_{sk}\end{aligned} \tag{3}$$

$\nu_{k'k}$ is the frequency at which collisions with big grains change the charge on a small grain from $k'\, e$ to $k\, e$. The $\nu_{k'k}$'s are considered in the next section. The continuity equation for the big grains is

$$\frac{\mathrm{d}}{\mathrm{d}z}(n_\mathrm{b}\, v_\mathrm{b}) = 0 \tag{4}$$

The charge on the big grains is followed with

$$\frac{\mathrm{d}}{\mathrm{d}z}(n_\mathrm{b}\, v_\mathrm{b}\, Z_\mathrm{b}) = n_\mathrm{b} \sum_k \Gamma_{sk\mathrm{b}}\, n_{sk} + n_\mathrm{b}\, (\Gamma_\mathrm{ib}\, n_\mathrm{i} + \Gamma_\mathrm{eb}\, n_\mathrm{e}) \tag{5}$$

Inertial terms in the force equations of the charged species are negligible. For an electric field $E\,\hat{z}$ the force equations of the various charged species may to a good approximation be taken to be

$$e\, E + m_\mathrm{i}\, \nu_\mathrm{in}\, (v_\mathrm{n} - v_\mathrm{i}) = 0 \tag{6}$$

$$-e\, E + m_\mathrm{e}\, \nu_\mathrm{en}\, (v_\mathrm{n} - v_\mathrm{e}) = 0 \tag{7}$$

$$m_\mathrm{b}\, g + Z_\mathrm{b}\, e\, E + m_\mathrm{b}\, \nu_\mathrm{bn}\, (v_\mathrm{n} - v_\mathrm{b}) = 0 \tag{8}$$

$$m_\mathrm{s}\, g + k\, e\, E + m_\mathrm{s}\, \nu_\mathrm{sn}\, (v_\mathrm{n} - v_{sk}) = 0 \tag{9}$$

$\nu_{j\mathrm{n}}$ is the collision frequency of species *j* with neutrals defined such that the time-averaged frictional force on a particle of species *j* due to collisions with neutrals is $m_j\, \nu_{j\mathrm{n}}\, (v_\mathrm{n} - v_j)$. We shall treat the $\nu_{j\mathrm{n}}$'s in the next section.

Neglect of the inertial terms in the force equations should be correct if the stopping length $v_j/\nu_{j\mathrm{n}}$ for a charged particle of species j due to its friction with neutrals is small compared to the scale lengths for the global variations arising from our numerical calculations. This condition should be always well fulfilled even for big grains for the parameters considered in this paper.

The electric field is governed by Poisson's equation

$$\frac{\mathrm{d}E}{\mathrm{d}z} = 4\pi e \left(n_\mathrm{i} - n_\mathrm{e} + n_\mathrm{b}\, Z_\mathrm{b} + \sum_k n_{sk}\, k \right) \tag{10}$$

3. Momentum transfer and charge transfer coefficients

The temperatures, T_j, of the various gaseous fluids are required to evaluate the momentum and charge transfer coefficients. As did Pilipp & Hartquist (1994) in a study of shocks in interstellar clouds, we neglect inertial terms in the equations governing the ion and electron temperatures. If we assume that the only energy transfer to or from the ions occurs via collisions between ions and neutrals that are elastic, the net energy transfer rate (e.g. Draine 1986) to or from the ions is zero if

$$T_\mathrm{i} = T_\mathrm{n} + \frac{m_\mathrm{n}\,(v_\mathrm{n} - v_\mathrm{i})^2}{3\,k_B} \tag{11}$$

which we will assume gives T_i (e.g. Pilipp & Hartquist 1994). k_B is Boltzmann's constant. If we equate the rate of energy transfer (e.g. Draine 1986) to electrons that occurs via collisions with neutrals that are elastic to the rate that electrons lose energy via the collisionally induced excitation of H_2 (e.g. Draine et al. 1983) we obtain T_e from

$$\left(\frac{8\,k_B\,T_\mathrm{e}}{\pi\,m_\mathrm{e}}\right)^{1/2} \sigma_\mathrm{en}\,k_B \left[\frac{8}{3}\,T_\mathrm{e}\,s_\mathrm{en}^2 \left(1+\frac{9\pi}{64}\,s_\mathrm{en}^2\right)^{1/2} + \left(\frac{m_\mathrm{e}}{m_\mathrm{n}}\right)(T_\mathrm{n}-T_\mathrm{e}) \left(4+\frac{8}{3}\,s_\mathrm{en}^2\right)\left(1+\frac{9\pi}{64}\,s_\mathrm{en}^2\right)^{1/2}\right] = 3\times10^{-23}\,\mathrm{erg\,cm^3\,s^{-1}\,K^{-1/2}}\,\frac{T_\mathrm{e}^{1/2}\,exp\left(-\frac{5987\,\mathrm{K}}{T_\mathrm{e}}\right)}{1+2994\,\mathrm{K}/T_\mathrm{e}} \tag{12a}$$

with

$$s_\mathrm{en}^2 = \frac{m_\mathrm{e}\,(v_\mathrm{n}-v_\mathrm{e})^2}{2\,k_B\,T_\mathrm{e}} \tag{12b}$$

$\sigma_\mathrm{en} \approx 1\times10^{-15}\mathrm{cm}^2$ (e.g. Massey 1969, p. 772). If (12a) yields $T_\mathrm{e} > 10^4\,\mathrm{K}$ then we set $T_\mathrm{e} = 10^4\,\mathrm{K}$ assuming that additional cooling processes for the electrons operate limiting the electron temperature accordingly. We specify T_n.

The momentum transfer rates between the gaseous neutral fluid and each of the other fluids is evaluated as described by Draine (1986). The momentum transfer rates between neutral gas particles and grains are appropriate for both totally elastic scattering with specular reflection and for totally inelastic scattering.

Expressions for the Γ_{jd}'s where j = i, e and d = b, sk are obtained straightforwardly from results given elsewhere (Havnes et al. 1987). They depend on the grain radius a_d, the grain charge, $\mid v_d - v_j \mid$, and T_j; we assume the sticking coefficients of electrons and ions with all grains to be unity except when we clearly state otherwise. Note that because the Γ_{jd}'s in this paper are the rate coefficients for the transfer of an elementary charge one obtains the $\Gamma_{\mathrm{e}d}$'s by multiplying the appropriate collision rate coefficients by -1.

We now focus on $\Gamma_{sk\mathrm{b}}$. We assume that $E > 0$, $v_\mathrm{n} > 0$, and $g < 0$ and consider the collision of a small grain carrying k elementary charges with a big grain. Θ is defined as the angle with respect to $\hat{z}$ of a vector from the center of the big grain to a point on the big grain's surface. If $v_\mathrm{b} < v_{sk}$ then the small grain can strike the big grain only at points at which $\pi/2 \le \Theta \le \pi$, and if $v_\mathrm{b} > v_{sk}$ the small grains strike the big grains surface only at points at which at which $0 \le \Theta \le \pi/2$. Usually for the cases considered in this study we have $v_\mathrm{b} < v_{sk}$. However, if the small grains attain sufficiently negative charges and a large enough electric field obtains $v_\mathrm{b} > v_{sk}$. In the following we derive the charge transfer coefficient $\Gamma_{sk\mathrm{b}}$ and the charge transfer frequency $\nu_{kk'}$ for $v_\mathrm{b} < v_{sk}$, but the derivation of the corresponding coefficients for cases in which $v_\mathrm{b} > v_{sk}$ is analogous. The surface charge density of the big grain before the collision is assumed to be

$$\sigma = \frac{3}{4\pi}\,E\,\cos\Theta + \frac{Z_\mathrm{b}\,e}{4\pi a_\mathrm{b}^2} \tag{13}$$

a_b is the radius of big grains. The change, δq_b, in the charge of a big grain in a collision with a small grain is assumed to be on average

$$\delta q_\mathrm{b} = k\,e - \left(\sigma + \frac{\delta q_\mathrm{b}}{4\pi a_\mathrm{b}^2}\right)\gamma\pi a_\mathrm{s}^2 - \delta Q_\mathrm{s}\,a_\mathrm{s} \tag{14a}$$

γ and δQ_s are introduced as free parameters describing the charge transfer in a big grain – small grain collision, and a_s is the radius of small grains. If we set $\delta Q_\mathrm{s} = 0$ and $\gamma = 2\pi^2/3$ (Latham & Mason 1962) Eq. (14a) would give the Elster-Geitel charge transfer taking place in a collision between a big perfectly conducting sphere and a small perfectly conducting sphere. In fact, the actual amount of charge transferred in such a collision depends on the ratio of the collision-contact time to the electrical relaxation time. In the real case, this number is so small as to make the inductive charge transfer negligible. In any event, as will become clear, inductive charge transfer is wholly inadequate for producing lightning – even in the idealized case of instantaneous electrical relaxation as is assumed here – and charge transfer must be dominated by assumed noninductive processes if lightning is to be possible.

δQ_s is the change of the electrostatic potential on a small grain due to noninductive charge transfer; various possible noninductive charging mechanisms are reviewed by Morfill et al. (1993). For example, the average charge transferred from a small grain per collision by non-inductive processes is one elementary charge for $\delta Q_\mathrm{s} = -4.802\times10^{-5}$ e.s.u. $= -1.44\times10^{-2}$ Volts and for a small grain radius $a_\mathrm{s} = 10^{-5}$ cm.

Clearly, since $a_s^2/a_b^2 << 1$

$$\delta q_b \approx k\,e - \sigma\,\gamma\pi a_s^2 - \delta Q_s\,a_s \tag{14b}$$

an approximation which we use everywhere in place of (14a). Thus,

$$\begin{aligned}\Gamma_{skb} &= \int_{\pi/2}^{\pi} (\delta q_b/e)\,(v_b - v_{sk})\,2\pi a_b^2\,\sin\Theta\,\cos\Theta\,d\Theta \qquad (15)\\ &\approx\ (v_b - v_{sk})\,\pi a_b^2\left[-k - \left(\frac{E}{2\pi e} - \frac{Z_b}{4\pi a_b^2}\right)\,\gamma\pi a_s^2 + \frac{\delta Q_s}{e}a_s\right]\end{aligned}$$

We now consider the $\nu_{k'k}$'s.

From the requirement of charge conservation it follows that if a small grain carrying the charge $k'\,e$ hits a big grain at an angle Θ the charge that the small grain carries away is on the average (as averaged over many collisions at the same angle Θ) equal to $k'\,e\ -\ \delta q_b$. However, in a particular big grain - small grain collision the small grain carries away an integral number of elementary charges rather than this average charge. In order to account for this fact we assume that the number of elementary charges that the small grain carries away is either k or $(k+1)$ where the integral number k is defined by $k\,e\ \le\ k'\,e - \delta q_b\ \le\ (k+1)\,e$ and where the probability for carrying away k elementary charges is $(k+1) - k' + \delta q_b/e$ and the probability for carrying away $(k+1)$ elementary charges is $k' - \delta q_b/e - k$.

In detail we proceed as follows:

We define

$$q_{su} \equiv \frac{Z_b\,e}{4\pi a_b^2}\,\gamma\pi a_s^2 + \delta Q_s\,a_s + e \tag{16a}$$

and

$$q_{sl} \equiv -\frac{3}{4\pi}\,E\,\gamma\pi a_s^2 + q_{su} - 2\,e \tag{16b}$$

We define Θ_k such that

$$\Theta_k = \pi \qquad \text{if} \qquad k < \frac{q_{sl}}{e} + 1 \tag{17a}$$

$$k\,e = \left(\frac{3}{4\pi}\,E\,\cos\Theta_k + \frac{Z_b\,e}{4\pi a_b^2}\right)\,\gamma\pi a_s^2 + \delta Q_s\,a_s$$

$$\text{if} \qquad \frac{q_{sl}}{e} + 1 \le k \le \frac{q_{su}}{e} - 1 \tag{17b}$$

$$\Theta_k = \frac{\pi}{2} \qquad \text{if} \qquad k > \frac{q_{su}}{e} - 1 \tag{17c}$$

We also define

$$q_s \equiv \left(\frac{3}{4\pi}\,E\,\cos\Theta + \frac{Z_b\,e}{4\pi a_b^2}\right)\,\gamma\pi a_s^2 + \delta Q_s\,a_s \tag{18}$$

From (13) and (14b) it follows that $q_s = k'\,e\ -\ \delta q_b$ with k' being the number of elementary charges which the small grain carries immediately before the collision with the big grain. Our assumptions for the number, k, of elementary charges which the small grain carries away after the collision can also be stated as follows:

- If a small grain collides with a big grain the number, k, of elementary charges that the small grain carries away lies between q_{sl}/e and q_{su}/e.
- If $q_{sl}/e + 1 \le k \le q_{su}/e - 1$ then there are two intervals in the angular range $\pi \ge \Theta \ge \pi/2$, defined by the grid points given by (17a) to (17c), where the small grains may carry away the charge $k\,e$ after collision. If the collision angle Θ is between $\Theta_{(k-1)}$ and Θ_k, then the probability that the small grain carries away a charge $k\,e$ is assumend to be $1 - k + q_s/e$; if the collision angle Θ is between Θ_k and $\Theta_{(k+1)}$, then the probability that the small grain carries away a charge $k\,e$ is assumed to be $1+k-q_s/e$. For Θ outside of these two intervals the probability for carrying away a charge $k\,e$ by the small grain is assumed to vanish.
- If $q_{sl}/e \le k < q_{sl}/e + 1$, then there is at most one interval of finite measure in the Θ range where the small grain may carry away a charge $k\,e$ after collision. That is, for $\pi \ge \Theta \ge \Theta_{(k+1)}$ the corresponding probability is assumed to be $1 + k - q_s/e$, but to vanish for $\Theta \le \Theta_{(k+1)}$. For intervals of zero measure given by $\Theta_{(k-1)} = \Theta = \Theta_k = \pi$ with $k < q_{sl}/e + 1$ we assume that the small grain carries away the charge $k_l\,e$ with the probability $k_l - q_{sl}/e$ where $q_{sl}/e \le k_l < q_{sl}/e + 1$.
- Analogously, if $q_{su}/e - 1 < k \le q_{su}/e$, there may be again at most one interval of finite measure in the Θ - range where the small grain may carry away the charge $k\,e$ after collision. That is, for $\Theta_{(k-1)} \ge \Theta \ge \pi/2$, the corresponding probability is assumed to be $1 - k + q_s/e$ but to vanish for $\Theta \ge \Theta_{(k-1)}$. For intervals of zero measure given by $\Theta_k = \Theta = \Theta_{(k+1)} = \pi/2$ with $k > q_{su}/e - 1$ we assume that the small grain carries away the charge $k_u\,e$ with the probability $q_{su}/e - k_u$ where $q_{su}/e - 1 < k_u \le q_{su}/e$.

Thus, with $k_l \le k \le k_u$,

$$\begin{aligned}\nu_{k'k} = &\\ &n_b \int_{\Theta_k}^{\Theta_{(k-1)}} [(1 - k + q_s/e)\,(1 - \delta_{k,k_l}) + (k_l - q_{sl}/e)\,\delta_{k,k_l}]\\ &\quad (v_b - v_{sk'})\,2\pi a_b^2\,\sin\Theta\,\cos\Theta\,d\Theta\\ &+ n_b \int_{\Theta_{(k+1)}}^{\Theta_k} [(1 + k - q_s/e)\,(1 - \delta_{k,k_u}) + (q_{su}/e - k_u)\,\delta_{k,k_u}]\\ &\quad (v_b - v_{sk'})\,2\pi a_b^2\,\sin\Theta\,\cos\Theta\,d\Theta\end{aligned}$$

where δ is the Kronecker δ, yielding for $k_l \le k \le k_u$

$$\begin{aligned}\nu_{k'k} = n_b\,(v_b - v_{sk'})\,\pi a_b^2 &\\ \times\{&[(q_{su}/e - k)\,(\cos^2\Theta_k - \cos^2\Theta_{(k-1)})\\ &+ \frac{E}{2\pi e}\,\gamma\pi a_s^2\,(\cos^3\Theta_k - \cos^3\Theta_{(k-1)})]\,(1 - \delta_{k,k_l})\\ &+ [(2 + k - q_{su}/e)\,(\cos^2\Theta_{(k+1)} - \cos^2\Theta_k)\\ &- \frac{E}{2\pi e}\,\gamma\pi a_s^2\,(\cos^3\Theta_{(k+1)} - \cos^3\Theta_k)](1 - \delta_{k,k_u})\} \qquad (19a)\end{aligned}$$

where (17a) and (17c) together with $k_\mathrm{l} < q_\mathrm{sl}/e + 1$ and $k_\mathrm{u} > q_\mathrm{su}/e - 1$ have been taken into account. For $k < k_\mathrm{l}$ or $k > k_\mathrm{u}$ we have

$$\nu_{k'k} = 0 \tag{19b}$$

Use of Eqs. (1), (2a), (3) through (5) and (15) and (19a), (19b) yields

$$\frac{\mathrm{d}J}{\mathrm{d}z} = 0 \tag{20a}$$

where J, the current, is given by

$$J = e\left(n_\mathrm{i}\, v_\mathrm{i} - n_\mathrm{e}\, v_\mathrm{e} + n_\mathrm{b}\, v_\mathrm{b}\, Z_\mathrm{b} + \sum_k n_{\mathrm{s}k}\, v_{\mathrm{s}k}\, k\right) \tag{20b}$$

Replacing (2a) by (2b) we get

$$\frac{\mathrm{d}(J\, +\, n_\mathrm{e}\, v_\mathrm{e})}{\mathrm{d}z} = 0 \tag{20c}$$

rather than (20a). Of course, $\sum_k n_{\mathrm{s}k}\, v_{\mathrm{s}k}$ is also a constant.

4. Numerical results

In the protosolar disk the gravitational forces due to the gravitational field of the Sun are largely balanced by the centrifugal forces of the orbiting medium. However, in a frame comoving with the gas of neutral molecules there is an effective gravitational field balancing the pressure gradients in the gas, i.e. the effective gravitational field is equal to the gas pressure gradient divided by the gas density. In this frame the grains are subjected to this effective gravitational field. For our model calculations we assume that there is some turbulent motion of the gas superimposed on its orbiting motion. We also assume that in a frame comoving with the orbiting gas motion the turbulent gas velocity is constant, at least within a certain distance range which is considered to be small compared to the thickness of the protosolar disk and for which we seek stationary solutions for the electric field. (See Weidenschilling & Cuzzi 1993 for likely length scales of turbulent motion).

We consider three sets of models. One consists of models for the protosolar nebula at a distance of 1 A.U. from the Sun and another is composed of models for the protosolar nebula at a distance of 5 A.U. (approximately the current radius of the Jovian orbit around the Sun). For any model belonging to either of these two sets we have assumed that the effective gravity is directed perpendicular to and towards the midplane of the protosolar nebula and that the turbulent neutral gas motion is away from it. The third set consists of models for the dust enriched subdisk. A dust enriched subdisk may be sufficiently thin that the effective gravitational force component perpendicular to the disk is weak relative to the effective gravitational force component in the radial direction. In models for a dust enriched subdisk we assume that the dominant component of the effective gravitational field is towards the Sun and the turbulent neutral motion is away from the Sun.

In all models, at $z = 0$ the following boundary conditions hold:

$$J = 0 \tag{21a}$$

$$E = 0 \tag{21b}$$

$$n_{\mathrm{s}k} = 0 \qquad \text{for} \quad k \neq 0, -1 \tag{21c}$$

At $z = 0$, Z_b is specified to be 0 except when we clearly state otherwise. The gas phase ion and electron number densities at $z = 0$ are given by the solution of Eq. (1) with the derivative set to zero and Eq. (2b), while $n_{\mathrm{s}-1}$ is simultaneously determined through the use of the condition that the total current is zero.

Table 1 gives the standard model parameters adopted for models in the three different sets considered.

The ionization rates ζ given in Table 1 are much lower than those usually assumed for molecular clouds if ionization is mainly provided by cosmic rays. We assume that during the formation of planets, the strong T-Tauri wind of the Sun has prevented ionizing cosmic rays from entering the solar system and that ionization is only due to decays of long-lived radioactive elements trapped in the grains (see Umebayashi & Nakano 1990). Thus, the ionization rates in Table 1 are lower limits.

The turbulent neutral velocity v_n given in Table 1 is about 5 per cent of the sound velocity $c_\mathrm{sound} = (7/5\, k_B\, T_\mathrm{n}/m_\mathrm{n})^{1/2}$ for the first column and about 11 per cent of the sound velocity for the second and third columns of the table. This is smaller than convection velocities suggested by early solar disk models but larger by about one order of magnitude for convective velocities derived from more recent analyses of convective instability modes in a rotating disk (for a review see Weidenschilling & Cuzzi, 1993). The value for the velocity of turbulent gas motion is very uncertain but could be as high as assumed by us, at least if extrinsic stirring mechanisms exist.

Since the grain fluxes $\sum_k n_{\mathrm{s}k}\, v_{\mathrm{s}k}$ and $n_\mathrm{b}\, v_\mathrm{b}$ are conserved (as can be derived from Eq. (3) and according to Eq. (4)) but the bulk grain velocities as well as the grain number densities or grain mass densities may vary with distance z, we adopt standard parameters for the grain mass densities at the boundary. In Table 1, standard parameters for the ratios of grain mass densities at a distance z to neutral mass density are expressed as the corresponding adopted ratios at the boundary times respective ratios χ_b and χ_s of grain bulk velocities at the boundary to respective grain bulk velocities ocurring at distance z.

Fig. 1 gives the electric field as a function of distance for several different models for conditions at 1 A.U. from the Sun. The upper curve, which is not marked, is for the standard parameters given in the first column of Table 1 and the boundary conditions given above. The curve marked EG_0 is for standard parameters, except $\delta Q_\mathrm{s} = 0$. The one marked EG_+ is for standard parameters except $\delta Q_\mathrm{s} = 0$ and at $z = 0, Z_\mathrm{b} = 10$. The curve marked $(\mathrm{EG}_0)_{\mathrm{S_{se}}=0.3}$ is for standard parameters except that $\delta Q_\mathrm{s} = 0$ and the electron sticking coefficients for small grains is 0.3 instead of unity. The thin horizontal lines at the right hand side of the figure indicate the electric field as derived numerically for the local equilibrium (i.e. all gradients in the

Table 1. Standard model parameters

	1 A.U.	5 A.U.	Dust Enriched
$\zeta\,(\mathrm{s}^{-1})$	1×10^{-22}	1×10^{-22}	1×10^{-20}
T_n (K)	750	150	150
$v_\mathrm{n}\,(\mathrm{km\,s}^{-1})$	0.1	0.1	0.1
$n_\mathrm{n}\,(\mathrm{cm}^{-3})$	1×10^{14}	1×10^{13}	2×10^{13}
$g\,(\mathrm{cm\,s}^{-2})$	-5×10^{-2}	-2×10^{-3}	-1×10^{-3}
a_b (cm)	0.1	0.1	0.1
a_s (cm)	1×10^{-5}	1×10^{-5}	1×10^{-5}
δQ_s (Volts)	-1.4406×10^{-2}	-1.4406×10^{-2}	-1.4406×10^{-2}
γ	1	1	1
$\rho_\mathrm{b}/\rho_\mathrm{n}$	$5\times10^{-3}\chi_\mathrm{b}$ [a])	$5\times10^{-3}\chi_\mathrm{b}$	$0.8\chi_\mathrm{b}$
$\rho_\mathrm{s}/\rho_\mathrm{n}$	$5\times10^{-3}\chi_\mathrm{s}$ [b])	$5\times10^{-3}\chi_\mathrm{s}$	$0.2\chi_\mathrm{s}$
$\rho_\mathrm{sp,b}\,(\mathrm{g\,cm}^{-3})$	1	1	1
$\rho_\mathrm{sp,s}\,(\mathrm{g\,cm}^{-3})$	1	1	1

[a] $\chi_\mathrm{b} \equiv (v_\mathrm{n} + g/\nu_\mathrm{bn})/v_\mathrm{b}$
[b] $\chi_\mathrm{s} \equiv (v_\mathrm{n} + g/\nu_\mathrm{sn})/v_\mathrm{s}$ with $v_s \equiv \sum_k n_{sk} v_{sk} / \sum_k n_{sk}$

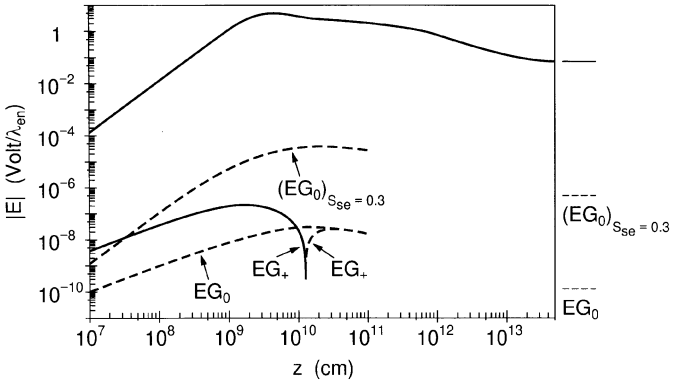

Fig. 1. The Electric Field as a Function of Distance for Models Appropriate for a Position at 1 A.U. from the Sun. Unless noted otherwise all parameters have the standard values given in the first column of Table 1 and the standard boundary conditions apply. The curves marked EG_0, EG_+, and $(\mathrm{EG}_0)_{\mathrm{S_{se}}=0.3}$ are for models with $\delta Q_\mathrm{s} = 0$. For the EG_+ case $Z_\mathrm{b} = 10$ at $z = 0$. For the $(\mathrm{EG}_0)_{\mathrm{S_{se}}=0.3}$ case the electron sticking coefficient on small grains was taken to be 0.3 rather than unity. Dashed portions of the curve indicate that the electric field is negative. $\lambda_\mathrm{en} \equiv 1/(\sigma_\mathrm{en}\, n_\mathrm{n})$. The thin horizontal lines at the right hand side of the figure indicate the electric field for the local equilibrium

equations and the current J defined by Eq. (20b) are zero) for each model. Appendix A treats the timescales for the generation of the electric field and for the attainment of ionization equilibrium while Appendix B concerns upper bounds and the equilibrium values of the electric field. Results in those appendices are relevant to the understanding of the numerical results displayed in Fig. 1 and other figures. Timescales are converted to the appropriate lengthscales by multiplication with v_n. (This is exact for the generation of electric field and is approximately true for attainment of ionization equilibrium of dust particles where $v_\mathrm{b} \approx v_{sk} \approx v_\mathrm{n}$, but does not necessarily hold for attainment of ionization equilibrium of ions and electrons because v_i and v_e deviate drastically from v_n for large magnitudes of the electric field. Only in case of the three marked curves in Fig. 1 corresponding to $\delta Q_\mathrm{s} = 0$, the ion and electron bulk velocities stay near v_n due to the very low electric field strengths. Note that in case of the curve marked $(\mathrm{EG}_0)_{\mathrm{S_{se}}=0.3}$ the time scale τ_e as given by (A12) must be multiplied by the factor $1/0.3$ since in the Appendices all sticking coefficients are assumed to be unity but lower electron sticking factors for small grains yield lower recombination rates for electrons increasing τ_e).

The physical processes operating to produce the electric field variations can be described as follows:

As argued in Appendix A the total current J can be decomposed into a sum of several partial currents: 1) the convection current $e\,Q\,v_\mathrm{n}$, where $e\,Q$ is the total space charge density (Q is defined by (A1)), 2) the current $e\,n_\mathrm{b}\,Z_\mathrm{b}\,g/\nu_\mathrm{bn}$ due to the movement of the charged big grains as seen in the rest frame of the neutrals which would occur if the only forces to which the big grains were subjected were gravity and friction with the neutrals, 3) the current $e\,(\sum_k n_{\mathrm{s}k}\,k)\,g/\nu_\mathrm{sn}$ due to the movement of charged small grains as seen in the rest frame of the neutrals which would occur if the only forces to which the small grains were subjected were gravity and friction with the neutrals, and 4) the conduction current $E\,/\,(4\pi\,\tau_\mathrm{E})$ containing the response of all charged particles to the external electric field E with the time scale τ_E defined by (A4).

Right at the boundary $z = 0$ (not shown in the figure where results are presented only for $z \geq 10^7$cm) we have $E = 0$ and $J = 0$.

In the case of the upper curve corresponding to standard parameters and standard boundary conditions, at $z = 0$ the only charged particles are ions, electrons and few charged small grains carrying one negative elementary charge. Then, from

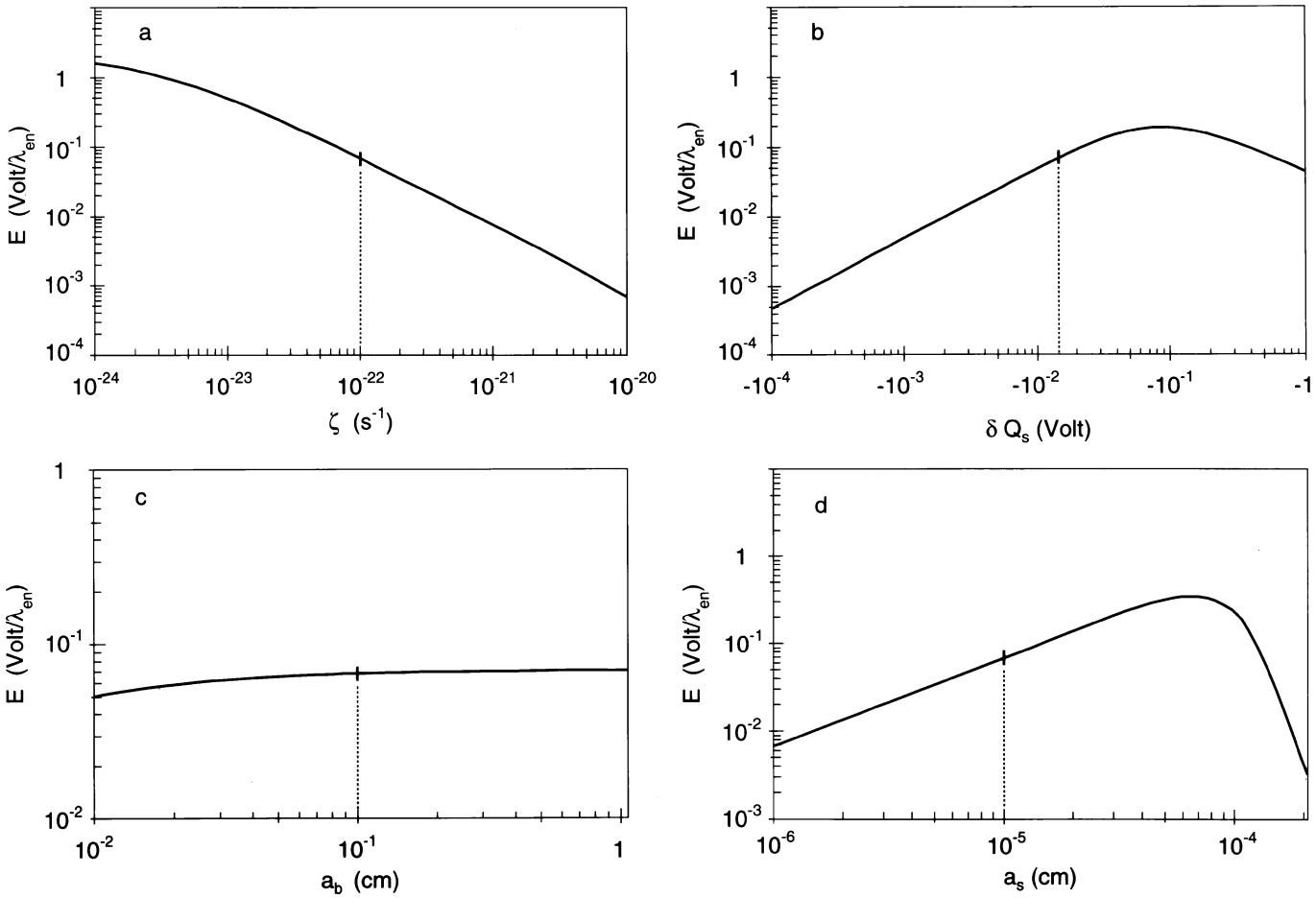

Fig. 2a–d. Local Equilibrium Values of the Electric Field for Models Appropriate for a Position at 1 A.U. from the Sun. All independent parameters, except the one on an axis in each panel are the standard ones. In each panel, the electric field dependence on the value of the one varied independent parameter is shown. The dashed lines mark the electric field when all independent parameters have the standard values

(A3) it follows that if $g < 0$ then $Q < 0$ producing according to Poisson's equation a negative electric field E as the medium moves to distances $z > 0$. However, at the same time as the medium moves upward, the big grains are charged positively in collisions with small grains and small grains colliding with big grains are charged negatively due to noninductive charge transfer. This effect results in a positive total charge density for distances z beyond 10^7cm but for distances not much larger than 10^9cm. Here, the positive charge density $e\,n_\mathrm{b}\,Z_\mathrm{b}$ for big grains and the negative charge density $e\,(\sum_k n_{sk}\,k)$ for small grains are about of the same magnitude but since ν_bn is smaller than ν_sn by 4 orders of magnitude the positive charge density of big grains dominates in accordance with (A3). In the distance range $10^7\mathrm{cm} \le z \le 10^9\mathrm{cm}$ we have roughly a balance between the convection current $e\,Q\,v_\mathrm{n}$ and the current $e\,n_\mathrm{b}\,Z_\mathrm{b}\,g\,/\,\nu_\mathrm{bn}$ of charged big grains whereas the other currents are of minor importance.

For distances significantly beyond 10^9cm the conduction current $E\,/\,(4\pi\,\tau_\mathrm{E})$ can no longer be neglected and eventually leads to a negative charge density at large distances. For distances near where the electric field reaches maximum and for distances beyond, variation of the electric field can be approximately described by the balance between the conduction current $E\,/\,(4\pi\,\tau_\mathrm{E})$ and the current $e\,n_\mathrm{b}\,Z_\mathrm{b}\,g\,/\,\nu_\mathrm{bn}$ of charged big grains as given by (B3) (see Appendix B for more details). In accordance with (A13) to (A16) the positive charge on big grains increases nearly linearly with z up to a distance $\sim v_\mathrm{n}\tau_\mathrm{bs} = 6 \times 10^9$cm and then approaches a local charge equilibrium approximated by (A15) (i.e. the gradient in (5) vanishes) at distances $\gg v_\mathrm{n}\tau_\mathrm{bs}$. In fact, the local equilibrium charge of big grains is slightly lower than given by (A15) due to electron impact not being taken into account in (A15). Most of small grains hitting big grains are discharged in the collisions if the big grains carry a charge near their local equilibrium charge because, in this case, the value of the average charge q_s carried away by small grains is small compared to one elementary charge (see also (18)) but grains can carry only an integral number of elementary charges. A small fraction of small grains hitting the big grains carry away one negative elementary charge since q_s is negative, and there are no small grains carrying away a charge different from either zero or one negative elementary charge, at least for electric field strengths not much larger than considered

in this paper for which electrostatic polarization of grain material is negligible. In this case, small grains are charged positively by ion impact and they are charged negatively by electron impact and by collisions with big grains and they are mainly discharged by collisions with big grains. Thus, the number densities of both positively and negatively charged small grains increase significantly with distance up to about $v_n \tau_{sb} = 1.5 \times 10^{13}$ cm but approach local charge equilibrium (i.e. vanishing gradients in (3)) at distances much larger than that distance in accordance with (A18).

The decay of the electric field beyond its maximum is caused by the increase of the charge on big grains and the increase of the number densities of charged small grains increasing the electrical conductivity of the medium. Whereas for small distances (i.e. for $z \leq 5 \times 10^8$cm) the electrical conductivity is dominated by gas phase ions and electrons, charged grains contribute the largest share to the electrical conductivity at the maximum of the electric field and for distances beyond of it. For distances $> 3 \times 10^{11}$cm small charged grains dominate the electrical conductivity of the medium and increase of their number densities with distance dominates the decay of the electric field accordingly. For local charge equilibrium as it should occur at distances $\gg v_n \tau_{sb}$ the electric field eventually reaches its equilibrium value which has been numerically determined to be about 6.8×10^{-2} Volts$/\lambda_{en}$.

The total current J is negligible compared to the current $e\, n_b\, Z_b\, g\, /\, \nu_{bn}$ although it does not vanish for all distances in spite of $J = 0$ at the boundary. The main reason for a finite total current is that for the upper curve in Fig. 1 (and also for the curves in Figs. 3, 4a, 5, and 6) we calculate the electron number density from (2b) rather than from (2a) as mentioned in Sect. 2 leading to (20c) rather than to (20a). That is, $J + n_e v_e$ is conserved so that $J = -n_e v_e + n_{e0} v_n$ with n_{e0} being the number density of gas phase electrons at the boundary. For $J > 0$, as should be the case for $E > 0$, the total current J increases the electric field according to Eq. (A3). However, for distances close to and beyond the maximum in E, the total current is smaller than the sum $S = \mid e\, Q\, v_n + e\, n_b\, Z_b\, g\, /\, \nu_{bn} + e\, (\sum_k n_{sk}\, k)\, g / \nu_{sn} \mid$ by two orders of magnitude or more so that the electric field is only slightly affected by the finite total current there. Only for small distances, i.e. $z < 10^8$cm, it is found that J is larger than S, by a factor of order unity.

For the curves marked EG_0 and $(EG_0)_{S_{se}=0.3}$, the boundary conditions are the same as those for the upper curve, again implying a negative space charge density at $z = 0$. However, in contrast to the upper curve, the big grains are charged negatively in collisions with other charged particles as the medium moves upward resulting in a negative total charge density for distances z beyond 10^7cm but not much larger than 10^{10}cm, and consequently in a negative electric field. Similarly as for the case of standard parameters (upper curve), the number density of charged small grains increases with distance due to ion and electron impact but here the electrical conductivity is dominated by gas phase ions and electrons for distances ranging from the boundary up to the distance where the maximum of the electric field strength occurs and is about constant in this distance range. Only at distances well beyond the maximum electric field strength (i.e. for $z > 10^{11}$cm) do the charged small grains contribute the largest share to the electrical conductivity decreasing τ_E significantly whereas contribution of the charged big grains to τ_E is always neglibible. Since here the electric field is in the negative direction, the effect of the conduction current is to increase space charge density according to (A3) and eventually produces a positive space charge density at large distances. The magnitude of the electric field shown by the curve marked $(EG_0)_{S_{se}=0.3}$ is higher than that shown by the curve marked EG_0 because for the smaller electron sticking coefficients for small grains the recombination rate of electrons is smaller resulting in a larger electron number density. As a consequence electron impact on grains is increased so that big grains for which the electron sticking coefficient is still assumed to be equal to one gain a negative charge of larger magnitude implying a larger magnitude of negative space charge density according to (A3). Finally, the positive electric field at small distances for the case corresponding to the curve marked EG_+ is a consequence of positive charge on big grains prescribed at $z = 0$. As can be seen from Fig. 1 both curves marked EG_0 and EG_+ end up in the same negative electric field at distances beyond 5×10^{10}cm so that evolution of the electric field at large distances does not depend on the boundary conditions.

The three marked curves had to be truncated beyond their maxima at about $z = 10^{11}$cm since numerical solution of Poisson's equation proved to be difficult beyond that distance. However, the local equilibrium electric fields which are expected to occur at sufficiently large distances were numerically derived also for these cases. We find a local equilibrium electric field $E \approx -1.3 \times 10^{-10}$ Volts$/\lambda_{en}$ for EG_0 and $E \approx -5.4 \times 10^{-7}$ Volts$/\lambda_{en}$ for $(EG_0)_{S_{se}=0.3}$. Also here, the electrical conductivity is dominated by the charged small grains when local equilibrium obtains. For each of these curves the decay of the electric field from the respective maximum absolute values near $z = 10^{11}$cm down to the respective absolute values for local equilibrium is mainly due to the increase of number densities of charged small grains as the medium moves upward.

In Fig. 2 results are given for the local equilibrium value of E (i.e. gradients and the total current J are zero). For each panel all input parameters but one have their standard 1 A.U. values; the value of this one input parameter varies and the dependence of the equilibrium value of E on it is explored. The question of whether local equilibrium might ever obtain arises. The scaleheight of the protosolar nebula at 1 A.U. was probably less than 10^{13} cm and results displayed in Fig. 1 (as well as in Fig. 3 and additional results shown in Fig. 4a below) are only meaningful for values of z somewhat less than that scaleheight and local equilibrium was never obtained if the assumed boundary conditions are the correct ones. However, it is possible that a closed cyclic convective flow was maintained for many turnover times, that the assumed boundary conditions were not the relevant ones, and that conditions in the flow evolved to approach local equilibrium. As described in the appendices the longest timescale in the evolution of the electrodynamic properties of our protosolar nebula models is the timescale for small

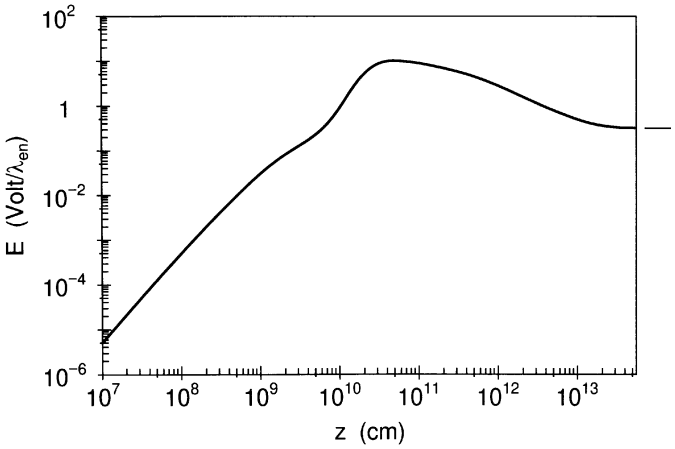

Fig. 3. The Electric Field as a Function of Distance for a Further Model Appropriate for a Position at 1 A.U. from the Sun. Results are for $a_s = 5 \times 10^{-5}$ cm. All other parameters have the values given in the first column of Table 1, and all boundary conditions are the standard ones. The thin horizontal line at the right hand side of the figure indicates the electric field for the local equilibrium

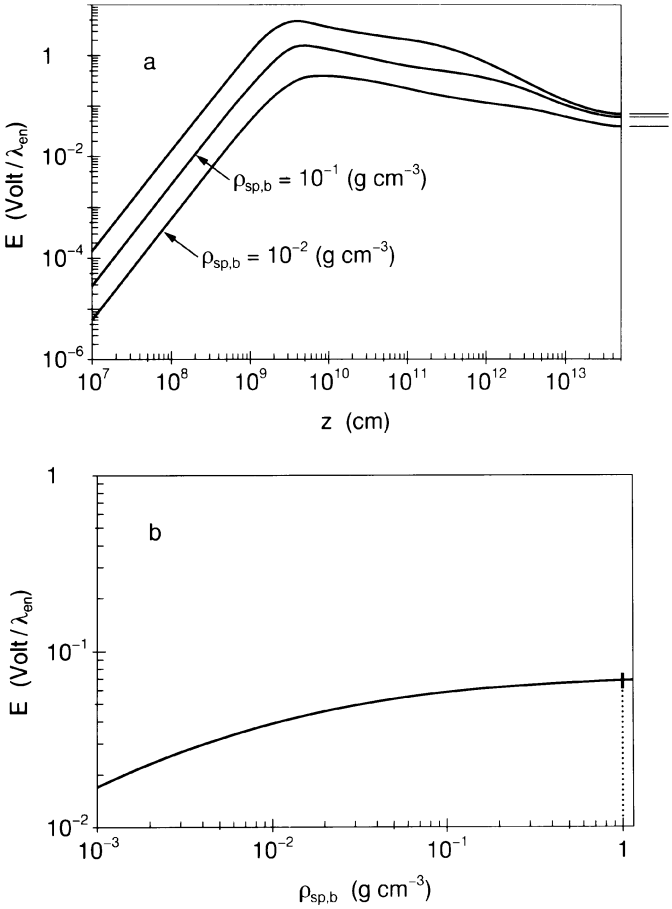

Fig. 4a and b. The Electric Field for Further Models Appropriate for a Position at 1 A.U. from the Sun. The density of the material of which the big grains is composed, $\rho_{sp,b}$, is varied and the radius of the big grains is assumed to be $0.1\mathrm{cm}\,(\rho_{sp,b}/1\mathrm{g\,cm^{-3}})^{-1/3}$. All other parameters have the values given in the first column of Table 1. **a** The electric field as a function of distance. The curves marked $\rho_{sp,b} = 10^{-1}\,(\mathrm{g\,cm^{-3}})$, $\rho_{sp,b} = 10^{-2}\,(\mathrm{g\,cm^{-3}})$, are for models for which the specific mass density of big grains has the indicated value. The upper curve which is not marked is for the standard parameter $\rho_{sp,b} = 1\,(\mathrm{g\,cm^{-3}})$, (i.e. the same curve as the upper curve in Fig. 1) and is given for comparison. The thin horizontal lines at the right hand side of the figure indicate the respective electric field for the local equilibrium. **b** Local equilibrium values of the electric field where $\rho_{sp,b}$, is the independent variable. As in Fig. 2 the dashed line marks the electric field for the standard choice of the independent parameter which is $\rho_{sp,b} = 1\mathrm{g\,cm^{-3}}$

grains to reach local charge equilibrium, and once a particular ion, electron, big grain, and small grain charge distribution is established the timescale for the growth of the electric field is very short compared to the turnover timescale. (In Sect. 5 we will comment on the question whether electric field strengths strong enough to induce lightning can be built up for local equilibrium.) As the numerical results given in Fig. 1 (and in Figs. 3, 5, and 6 and additional results in Fig. 4a) and considerations presented in the appendices show the largest electric field strengths obtain if the big grains have had time to charge up but the small grain charge distribution has not approached local equilibrium; thus, a particular range of lifetimes of convective cells would favour the generation of electric fields strong enough to induce discharge.

As is argued in Appendix B variation of the local equilibrium electric field with various relevant parameters can be approximated by (B8) if the parameters are near the standard ones. (B8) results from the balance between the conduction current $E\,/\,(4\pi\,\tau_E)$ and the current $e\,n_b\,Z_b\,g\,/\,\nu_{bn}$ of charged big grains as given by (B3) if Z_b can be approximated by (A15) and τ_E can be approximated by τ_{Es} with τ_{Es} given by (A21). The conditions on which these approximations are based are detailed in Appendix C. The most important conditions are that 1) the electrical conductivity of the medium is dominated by charged small grains, the small grains are in local charge equilibrium and most of the charged small grains carry one positive or one negative elementary charge so that higher charge states of the small grains can be neglected and that 2) the charge on big grains is in local equilibrium and is mainly determined by noninductive charge exchange and electrostatic relaxation from collisions between big grains and small grains.

For Fig. 2a, (B8) holds for $3 \times 10^{-24}\,\mathrm{s^{-1}} \leq \zeta \leq 10^{-21}\,\mathrm{s^{-1}}$ where the decrease of E with increasing ζ is due to $\tau_{Es} \sim \zeta^{-1}$ (see (A21)). The decrease of τ_{Es} results from the increase of the number density of charged small grains with increasing ζ (see(A17)) which in turn results from the increase of the number densities of gas phase ions and electrons implying an increased production rate for charged small grains.

(B8) breaks down for $\zeta \leq 10^{-24}\,\mathrm{s^{-1}}$ and for $\zeta \geq 10^{-21}\,\mathrm{s^{-1}}$ because in the lower range of ζ charged big grains and in the higher range of it higher charge states of small grains become important for τ_E.

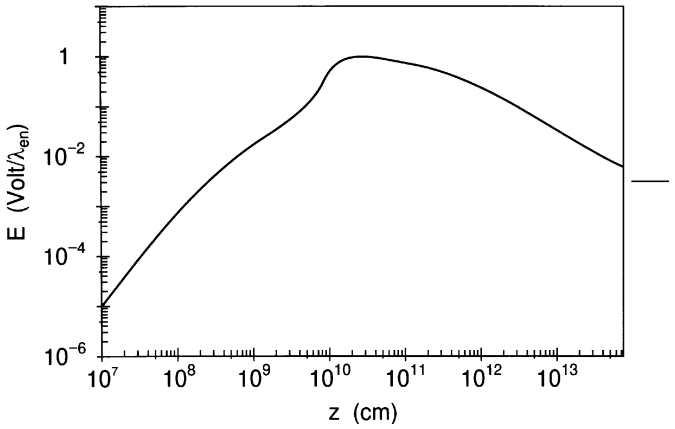

Fig. 5. The Electric Field as a Function of Distance for a Model Appropriate for a Position at 5 A.U. from the Sun. All parameters have the values given in the second column of Table 1. The boundary conditions are the standard ones. The thin horizontal line at the right hand side of the figure indicates the electric field for the local equilibrium

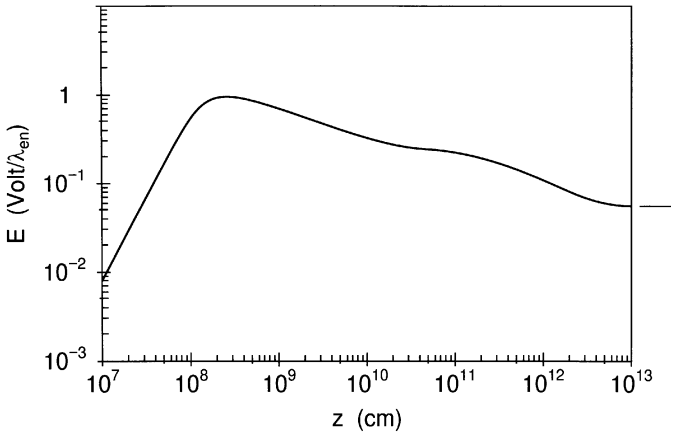

Fig. 6. The Electric Field as a Function of Distance for a Model Appropriate for a Dusty Subdisk. All parameters have the values given in the third column of Table 1. The boundary conditions are the standard ones. The thin horizontal line at the right hand side of the figure indicates the electric field for the local equilibrium

For Fig. 2b, (B8) holds at least for $|\delta Q_s| \leq 4 \times 10^{-2}$ Volts where the increase of E with increasing $|\delta Q_s|$ is due to $Z_b \sim |\delta Q_s|$ (see (A15)).
(B8) becomes questionable for $|\delta Q_s| > 4 \times 10^{-2}$ Volts because the electric field significantly decreases $v_n - v_b$ and, as a consequence, τ_{Es} becomes smaller than given by (A21). For $|\delta Q_s| > 1 \times 10^{-1}$ Volts (B8) breaks down because charged big grains dominate τ_E there, i.e. the electric field approaches E_b as defined by (B5) where gravitational forces and electrostatic forces on the big grains balance.

For Fig. 2c, (B8) holds for the total parameter range considered where E is about constant due to $Z_b \sim a_b^2$ (see (A15)) and $\rho_b/(m_b\,\nu_{bn}) \sim a_b^{-2}$ so that the current of charged big grains moving downward in the rest frame of neutrals does not vary with a_b.

For Fig. 2d, (B8) holds for $10^{-6}\,\mathrm{cm} \leq a_s \leq 2 \times 10^{-5}\,\mathrm{cm}$ where the increase of E with increasing a_s is due to $Z_b \sim a_s^{-1}$ (see (A15)) and $\tau_{Es} \sim a_s^2$ (see (A21)). The increase of τ_{Es} with a_s results from $m_s\,\nu_{sn} \sim a_s^2$ (see also A7), i.e. from a decrease of mobility of small grains with increasing size whereas the number density of charged small grains does not vary with a_s (see (A17)).
(B8) breaks down for $a_s \geq 2 \times 10^{-5}$cm because there higher charge states of small grains become important for τ_E, and for $a_s \geq 10^{-4}$cm gas phase ion and electron number densities become so high due to reduction of recombination on small grain surfaces that gas phase ions start to dominate the electical conductivity of the medium and, in addition, electron impact on big grains reduce the positive charge on them drastically so that Z_b decreases with a_s much faster than predicted by (A15).

As seen from Fig. 2d the local equilibrium electric field strength is larger for $a_s = 5 \times 10^{-5}$cm than for $a_s = 1 \times 10^{-5}$cm. Thus, Fig. 3 shows results for the dependence of the electric field when $a_s = 5 \times 10^{-5}$cm. All other parameters have the values given in the first column of Table 1, and all boundary conditions are the standard ones. Also here, the thin horizontal line at the right hand side of the figure indicates the electric field for the local equilibrium.

It should be mentioned that for Fig. 3 the ratio of the total current *J* to the sum *S* is much larger than for the upper curve in Fig. 1 for distances close to and beyond the maximum electric field, so that E is more strongly affected by the total current there. This difference results mainly from the fact that if the small particles are larger, the total current $J = -n_e v_e + n_{e0} v_n$ is increased as a result of the increase of both n_e and $\mid v_e \mid$, and that the current of the charged big grains $\mid e\,n_b\,Z_b\,g\,/\,\nu_{bn} \mid$ is lowered as a result of the decrease of Z_b. Our numerical results show that the total current *J* is never larger than half the current $\mid e\,n_b\,Z_b\,g\,/\,\nu_{bn} \mid$ and is significantly smaller than the sum *S* for distances $z \geq 10^9$ cm. The ratio J/S shows a local maximum of about 0.55 at the distance $z = 2 \times 10^{10}$ cm and is about 0.3 at $z = 5 \times 10^{10}$ cm, where E reaches its maximum. That is, there is a moderate effect of *J* on E, increasing the maximum electric field strength by a factor of about 1.3. In summary, we conclude that increasing the radius a_s of small grains from the standard value of 10^{-5} cm to 5×10^{-5} cm increases the maximum electric field strength roughly by a factor 2. At large distances, i.e. $z \gg v_n \tau_{sb} = 1.5 \times 10^{13}$ cm, the electric field shown in Fig. 3 approaches its local equilibrium value as calculated by setting gradients and *J* equal to zero (indicated by the thin horizontal line at the right hand side of the figure).

Fig. 4 gives results for the electric field E for models appropriate for a position at 1 A.U. from the Sun, when the mean specific mass density of the big grains is varied but their mass is kept constant at $(4\pi/3) \times 10^{-3}$g. Very low mean specific mass densities correspond to very porous grains. Again, all other input parameters have their standard values given in the first column of Table 1, and all boundary conditions are the standard ones. Fig. 4a gives the electric field as a function of distance for specific mass densities of 10^{-1} (g cm^{-3}) and of 10^{-2} (g cm^{-3}) as indicated at the corresponding curves. The upper curve, which

is not marked, is the same as the upper curve in Fig. 1, corresponding to standard 1 A.U. parameters (Table 1). The thin horizontal lines at the right hand side of the figure indicate the respective electric field for the local equilibrium.

Fig. 4b gives results for the local equilibrium value of E for a larger range of values for the parameter $\rho_{\mathrm{sp,b}}$. For Fig. 4b, (B8) holds nearly for the total parameter range considered where E is about constant due to similar reasons as for Fig. 2c, except for $\rho_{\mathrm{sp,b}} \leq 10^{-2}\,\mathrm{g\,cm^{-3}}$ where reduction of τ_{E} by charged big grains becomes significant.

From Fig. 4a it can be seen that the electric field strength is generally reduced when $\rho_{\mathrm{sp,b}}$ decreases. This reduction of the electric field strength is predominantly a transient effect which becomes less significant for large distances where the medium approaches local equilibrium in accordance with Fig. 4b. As can be seen from Eq. (A16) in Appendix A, the time scale τ_{bs}, which is the time scale for big grains to reach their equilibrium charge (as given by (A15)) increases with decreasing $\rho_{\mathrm{sp,b}}$ when simultaneously $a_{\mathrm{b}} \sim \rho_{\mathrm{sp,b}}^{-1/3}$ (= constant grain mass). In addition, the absolute value of the average charge q_{s} (with $q_{\mathrm{s}} < 0$) carried away by the small grains in collisions with big grains increases when Z_{b} is reduced relative to its equilibrium value (see Eq. (18)), resulting in a larger number of charged small grains and a higher electrical conductivity. These are the two prime effects responsible for the decrease of the electric field during the transient phase.

As for the upper curve in Fig. 1 the total current is negligible at least for distances $z \geq 3 \times 10^8$cm and affects the electric field by a factor of only order unity for smaller distances.

Fig. 5 displays the electric field as a function of distance for the conditions that obtained in the protosolar nebula at what is presently Jupiter's orbit (5 A.U.). The curve is for the standard 5 A.U. parameters listed in Table 1 and the standard boundary conditions. The scale height of the nebula was probably less than 10^{13}cm. The thin horizontal line at the right hand side of the figure again indicates the electric field for the local equilibrium.

Here, the effect of the total current on the electric field is again small at least for distances $z \geq 3 \times 10^8$cm although it is larger than for the conditions of Figs. 1 and 4a. It is of order unity for smaller distances. The ratio of the total current J to the sum S shows a local maximum of about 0.2 at the distance $z = 2 \times 10^{10}$ cm and it is about 0.1 at $z = 2.7 \times 10^{10}$ cm where E reaches its maximum so that the current J should increase the maximum electric field by a factor 1.1.

The curve in Fig. 6 gives the electric field as a function of distance for the standard parameters for the dust enriched subdisk in Table 1 and standard boundary conditions. The radial extent of the subdisk may have been as much as almost 10^{14}cm, but its thickness was probably about 10^{12}cm or less (Dubrulle et al. 1995). The thin horizontal line at the right hand side of the figure, as usual, indicates the electric field for the local equilibrium. Here, the effect of the total current J on the electric field is negligible everywhere.

The physical processes operating to produce the electric field variations as shown in Fig. 3, by the two lower curves in Fig. 4a, and in Figs. 5 and 6 are qualitatively similar to those discussed for the upper curve in Fig. 1 although quantitative details are different. As is the upper curve in Fig. 1, the curves in Figs. 3, 4a and 6 are plotted up to distances well beyond $v_{\mathrm{n}}\tau_{\mathrm{sb}}$ (i.e. well beyond 1.5×10^{13} cm for Figs. 1, 3, 4a and 2×10^{12} cm for Fig. 6) where the electric field almost reaches local equilibrium. However, the curve shown in Fig. 5 is not plotted up to a distance beyond $v_{\mathrm{n}}\tau_{\mathrm{sb}}$, which here is 1.7×10^{14} cm, because numerical solution proved to become difficult beyond 7.5×10^{13} cm. Therefore, the curve is still significantly above the local equilibrium value of the electric field at the largest distances shown in the figure.

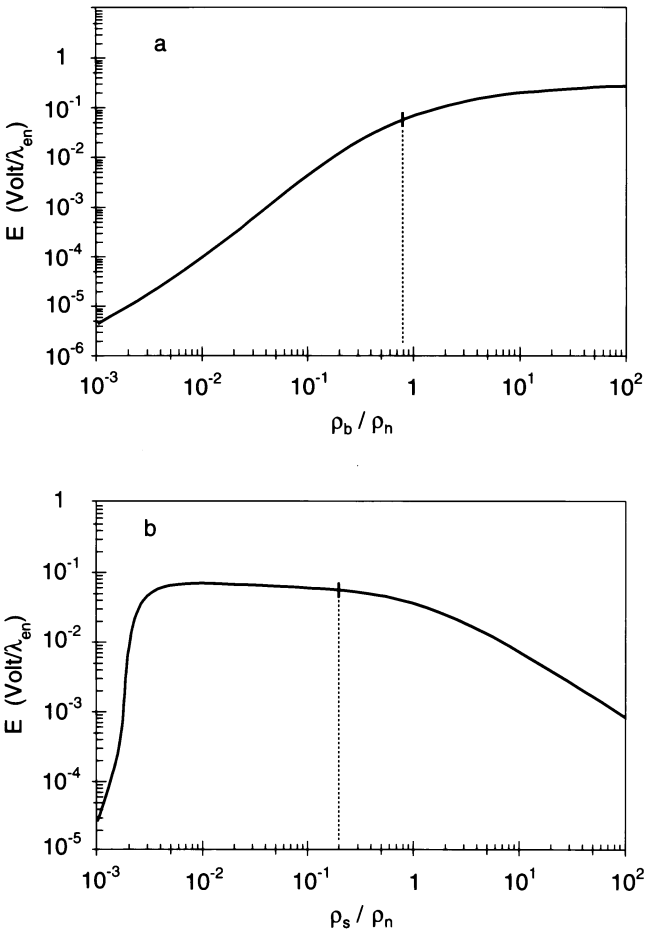

Fig. 7a and b. Local Equilibrium Values of the Electric Field for Models Appropriate for a Dusty Subdisk. In panel **a** $\rho_{\mathrm{b}}/\rho_{\mathrm{n}}$ is the independent variable; in panel **b** $\rho_{\mathrm{s}}/\rho_{\mathrm{n}}$ is the independent variable. For results in both panels $\zeta = 1 \times 10^{-20} s^{-1}$ $((\rho_{\mathrm{b}} + \rho_{\mathrm{s}})/\rho_{\mathrm{n}})$. All other parameters have the standard values given in the third column of Table 1. Just as in Figs. 2 and 4b the dashed lines indicate the result obtained when all input parameters have their standard values

Fig. 7 shows the local equilibrium electric field for models appropriate for a dusty subdisk. The ratio $\rho_{\mathrm{b}}/\rho_{\mathrm{n}}$ is the independent variable in panel a, and the ratio $\rho_{\mathrm{s}}/\rho_{\mathrm{n}}$ is the independent variable in panel b. $\zeta = 1 \times 10^{-20}\mathrm{s}^{-1}$ $((\rho_{\mathrm{b}} + \rho_{\mathrm{s}})/\rho_{\mathrm{n}})$ is assumed. All other parameters have the standard values in column 3 of Table 1.

For Fig. 7a, (B8) is fulfilled when roughly $0.1 \leq \rho_b/\rho_n \leq 2$, where the increase of E with increasing ρ_b/ρ_n results largely from the increase of the current $e\, n_b\, Z_b\, g\, /\, \nu_{bn}$ of charged big grains as $\sim \rho_b/\rho_n$ (for $Z_b \approx const.$) and, in addition, when $\rho_b/\rho_n \leq 0.7$ from the increase of τ_{Es}. The increase of τ_{Es} is caused by the increase of the rate of discharging for small grains due to collisions with big grains with increasing ρ_b/ρ_n decreasing the number density of charged small grains in spite of the fact that ζ also increases with ρ_b/ρ_n. However, the increase of τ_{Es} with increasing ρ_b/ρ_n as predicted by (A21) becomes neglibible at $\rho_b/\rho_n > 1$ as, at the same time, ζ increases nearly as $\sim \rho_b/\rho_n$. In fact, τ_{Es} even slightly decreases with increasing ρ_b/ρ_n at $\rho_b/\rho_n > 0.7$ probably because there the decrease of $v_n - v_b$ with the increase of the electric field results in a decrease of the discharging rate for small grains as compared to what is expected if electric forces are neglected for determining $v_n - v_b$. (B8) breaks down for $\rho_b/\rho_n < 0.1$ and $\rho_b/\rho_n > 2$ where the electric field as shown in Fig. 7a is larger in the first range and smaller in the second range than that estimated by (B8). For very small values of ρ_b/ρ_n the assumptions for estimating the number densities of charged small grains by (A17) break down, mainly because here small grains are discharged also significantly by ion and electron impact in addition to being discharged by collisions with big grains. For large numbers of ρ_b/ρ_n charged big grains dominate τ_E, i.e. the electric field approaches E_b as defined by (B5).

For Fig. 7b, (B8) is fulfilled when $\rho_s/\rho_n \geq 10^{-2}$, where the variation of E observed in the figure results from the variation of τ_{Es} with ζ as given by (A21) and the assumed variation of ζ with ρ_s/ρ_n whereas Z_b is roughly constant.
(B8) breaks down at $\rho_s/\rho_n \ll 10^{-2}$ because there number densities of gas phase ions and electrons become so large due to their small recombination rates that the positive charge on big grains is drastically reduced by electron impact and, at $\rho_s/\rho_n \leq 10^{-3}$ gas phase ions and electrons dominate the electrical conductivity of the medium.

5. Discussion

We assume that discharge occurs if the electric field strength is roughly one to several Volts$/\lambda_{en}$ (Pilipp et al. 1992) where $\lambda_{en} \equiv 1/(\sigma_{en}\, n_n)$; then a nonnegligible fraction of electrons have energies exceeding the ionization potential of the neutral gas. (However, the critical field strength for breakdown is uncertain, and Gibbard et al. 1997 advocate a higher value.) Inspection of the results presented in the figures in the previous section shows that discharges might have occurred in the protosolar nebula; however, according to Fig. 1 discharges occurred only if processes other than gas phase ion and electron collisions with grains and the Elster-Geitel mechanism also operated to charge the grains and local equilibrium did not obtain even if the ionization rate was low compared to the rates that obtain in interstellar clouds and approached the rate provided by the decay of K^{40} trapped in grains (e.g. Umebayashi & Nakano 1990).

Though charging mechanisms other than the Elster-Geitel effect may well have operated, the conclusion that lightning's existence in the protosolar nebula depended on the functioning of mechanisms that remain unidentified is an unsatisfying one.

We find from our calculations that polarization of the grains' surface charge distribution by the external electric field has a negligible effect on the charge transfer process. In fact, electrostatic polarization of the grain material produces only a small change of the surface charge density of big grains if $\mid E \mid \ll (1/3) \mid Z_b \mid (e/a_b^2)$ (see Eq. (13)) or if $\mid E \mid \ll 4.8 \times 10^{-5}\,\mathrm{Volts}/\lambda_{en} \mid Z_b \mid (a_b/(10^{-1}\mathrm{cm}))^{-2}\ (n_n/(10^{14}\mathrm{cm}^{-3}))^{-1}$, which has been found to be well fulfilled for all cases presented in the present paper, so that the charge δq_b transferred to a big grain in a big grain - small grain collision is not significantly affected by polarization (see Eqs. (13) and (14b)). Thus, we conclude that the Elster-Geitel mechanism is unimportant for charging of the grains in the protosolar nebula.

More important grain charging mechanisms result from impact of gas phase ions and electrons on the grains as well as electrostatic relaxation in big grain - small grain collisions which are the dominant grain charging mechanisms for the cases shown by the curves marked EG_0, EG_+ and $(EG_0)_{S_{se}=0.3}$ in Fig. 1.

However, as mentioned above, grain charging which is effective enough to generate electric fields capable of inducing lightning could occur only if additional charging mechanisms operate. Therefore, most of our results presented in this paper, except for the curves marked EG_0, EG_+ and $(EG_0)_{S_{se}=0.3}$ in Fig. 1, are based on the assumption that in big grain - small grain collisions non-inductive charge transfer processes occur which we describe by the free parameter δQ_s. For our standard parameter $\delta Q_s = -1.44 \times 10^{-2}$ Volts, big grains are charged positively as they move upward and reach a positive equilibrium charge at large distances which is mainly determined by the balance between gain of positive charge $-\delta Q_s\, a_s$ due to non-inductive charge transfer and loss of positive charge $-\sigma\, \gamma \pi a_s^2$ due to electrostatic relaxation (see Eq. (14b)). This results in an electric field being directed into the positive z-direction at least for distances $z \geq 10^7$ cm. The positive charge on the big grains is only slightly reduced by impact of gas phase electrons for input parameters having the standard 1 A.U. values or the standard values for the dust enriched subdisk. For input parameters having the standard 5 A.U. values electron impact reduces the charge on big grains also only slightly for distances up to $\approx 10^{13}$ cm but the positive charge on big grains is reduced significantly at large distances where the medium approaches local equilibrium. Additional charging processes for big grains due to the absorption of the charge $k\, e$ in a big grain - small grain collision (with $k\, e$ being the charge on the small grain before colliding with the big grain) and due to ion impact on the big grains are less important, at least for input parameters having values not considerably different from our standard values and for distances $z \geq 10^7$ cm. (See also Appendix C for a discussion of the relative importance of different grain charging mechanisms). Small grains are charged negatively in big grain - small grain collisions if the charge number Z_b for big grains is still significantly lower than that given by Eq. (A15), (see Eqs. (18)

and (A15)) and they are charged positively and negatively by collisions with gas phase ions and electrons. As Z_b approaches the equilibrium value given by Eq. (A15) for large distances in the case of 1 A.U. parameters and dust enriched subdisk standard parameters then small grains are charged mainly by ion and electron impact but are discharged mainly in collisions with big grains.

It should be mentioned that chondrule precursors were not spheres but were probably irregular fractal aggregates, whereas for our models we assume that the dust particles were spherical. Charges on such irregular bodies would produce highly nonuniform electric fields in the immediate neighborhood of the dust particles so that charge transfer would be unlike that expected for uniform spheres. However, for our model calculations we treat the non-inductive grain - grain charge transfer, which is mainly responsible for the generation of strong global electric fields, by the two free parameters δQ_s and γ which allow us to vary the charge on the big grains. The uncertainties which the assumption of spherical dust grains add to our treatment is therefore included in the uncertainties for the choice of these free parameters.

The question arises whether the strength of the global electric field E can be significantly enhanced, as compared to that derived from our standard parameters, if input parameters are varied. For example, increase of the absolute value of the free parameter δQ_s should result in a more effective charging of grains which should affect the generation of electric fields.

Figs. 2 and 4b show that, at least for a medium in local equilibrium, variation of several relevant parameters which could significantly deviate from our standard parameters given in the first column of Table 1 allow only a limited increase of the electric field. As expected, increase of the ionization rate decreases the electric field (see Fig. 2a), so that choosing the minimum ionization rate allowed by physical considerations should yield the maximum electric field strength. Increase of the absolute value of the parameter δQ_s can increase the electric field. However, there is a maximum at $\delta Q_s \approx -0.1$ Volts, and the electric field decreases again, if $\delta Q_s < -0.1$Volts (see Fig. 2b). An increase of the radius of small grains increases the electric field to a maximum value of about $0.34\,\mathrm{Volts}/\lambda_{en}$ at $a_s = 6.63 \times 10^{-5}$ cm. However, the electric field decreases drastically if a_s is increased above $a_s \geq 10^{-4}$ cm (see Fig. 2d). Finally, variation of the radius a_b and specific mass density $\rho_{sp,b}$ of big grains has only minor effects on the local equilibrium values of the electric field strength (see Figs. 2c and 4b).

Analogous to the plot presented in Fig. 2d, we also produced plots for the variation of the equilibrium electric field for the protosolar nebula at 5 A.U. distance from the Sun and for the dust enriched central disk where all input parameters but a_s have their standard values as given in the second and third column of Table 1, respectively, and where a_s is varied. These plots are not shown in the paper. We found that variation of the local equilibrium electric field with a_s for the models corresponding to 5 A.U. distance from the Sun and to the dust enriched central disk is largely similar to that shown in Fig. 2d:

In the case of the protosolar nebula at 5 A.U., the local equilibrium electric field strength increases with a_s up to a maximum of $1.8 \times 10^{-2}\,\mathrm{Volts}/\lambda_{en}$ at $a_s = 3.1 \times 10^{-5}$ cm but decreases rapidly with increasing a_s for $a_s > 4 \times 10^{-5}$ cm. The local equilibrium electric field strength is $3.6 \times 10^{-3}\,\mathrm{Volts}/\lambda_{en}$ at $a_s = 1 \times 10^{-5}$ cm, i.e. if all input parameters have their standard values. In the case of the dust enriched central disk, the local equilibrium electric field strength increases with a_s up to a maximum of $0.36\,\mathrm{Volts}/\lambda_{en}$ at $a_s = 8 \times 10^{-5}$ cm but decreases rapidly with increasing a_s for $a_s > 1.2 \times 10^{-4}$ cm.

Fig. 7a shows that an increase of the mass density ρ_b for the big grains leads to an increase in the local equilibrium electric field strength, up to $0.3\,\mathrm{Volts}/\lambda_{en}$ for a dust enriched central disk. In contrast, Fig. 7b shows that the local equilibrium electric field strength in this central plane does not vary strongly if the mass density ρ_s for the small grains is varied around its standard value within a wide range.

These results indicate that in most cases high electric field strengths capable of inducing lightning are not reached for local equilibrium conditions, although local equilibrium electric field strengths approaching the breakdown field have been found for a narrow range of parameters. (For example, for standard parameters appropriate for a distance of 1 A.U. as given in the first column of Table 1, except for the input parameters δQ_s and a_s, which were chosen as $\delta Q_s = -0.87 \times 10^{-1}$ Volts and $a_s = 5 \times 10^{-5}$ cm, we found a local equilibrium electric field strength of about $0.89\,\mathrm{Volts}/\lambda_{en}$.) If the small grains are far from local charge equilibrium, however, so that the electrical conductivity of the medium is much lower than that in local equilibrium, sufficiently high field strengths can be generated more easily.

We investigated also whether the electric field strength can be significantly increased by variation of input parameters if local equilibrium did not obtain.

In order to discuss the dependence of the electric field strength on δQ_s in more detail we consider mostly negative values for this input parameter. The reason for this is that for $\delta Q_s < 0$ and a sufficiently large magnitude for δQ_s (e.g. for our standard value $\delta Q_s = -1.44 \times 10^{-2}$Volts) the electric field generated by charge separation is directed into the positive z-direction at least for distances $z \geq 10^7$ cm so that the ions move always into that direction and Eq. (1) can be integrated numerically along that direction for all electric field strengths. In contrast, if we choose $\delta Q_s > 0$ then the resulting electric field is directed into the negative z- direction yielding $v_i < 0$ for large electric field strengths. In this case integration of Eq. (1) along the positive z-direction becomes unstable and then we have to replace Eq. (1) by an approximation for which the term $(\mathrm{d}/\mathrm{d}z)(n_i\, v_i)$ is neglected. We performed also calculations for $\delta Q_s = +1.44 \times 10^{-2}$ Volts, with all other input parameters having their standard values (for which figures are not shown in this paper). From these calculations we find that for all input parameters (except for, of course, δQ_s) having their standard 1 A.U. parameters, or their standard parameters for the dust enriched subdisk, the switch of the value for δQ_s from -1.44×10^{-2} Volts to $+1.44 \times 10^{-2}$ Volts causes only slight differences between the

curves for the variation of the absolute value of the electric field with distance. For the standard 5 A.U. parameters the deviations between corresponding curves for the absolute value of the electric field are significantly larger when the value for δQ_s is switched. However, both curves still agree at least within an order of magnitude. (For the distance range between 2×10^8 cm and 2×10^{10} cm these deviations are in part due to a major error caused by neglecting the term $(\mathrm{d}/\mathrm{d}z)(n_i\, v_i)$ in Eq. (1)). We expect from these results that variation of electric field strength can be fully investigated at least within an order of magnitude if we consider only negative values for δQ_s but for $\mid \delta Q_s \mid$ large enough to generate electric fields capable of inducing lightning.

A major effect of increase of $-\delta Q_s$ (as compared to its standard value) is that Z_b reaches a higher value (see Eqs. (5) and (15) and note that $v_b - v_{sk} \approx v_b - v_n < 0$, or see corresponding Eqs. (A13), (A15), (A16)). In addition, increase of $-\delta Q_s$ results also in an increase of the absolute value of the negative charge q_s carried away on the average by the small grains in big grain - small grain collisions if Z_b is still well below the value given by (A15) (see Eqs. (18) and (A15)). Finally, as a consequence of these changes of grain charges several additional mutual interactions as described by the equations in Sects. 2 and 3 between grains, gas phase ions, gas phase electrons, and the electric field change the ionization structure of the medium.

As discussed in Appendix B, the electric field E at the position z where E reaches a peak value and probably also at distances beyond this position can be approximately derived from a balance between the conduction current $E\,/\,(4\pi\,\tau_E)$ and the current $e\,n_b\,Z_b\,g/\nu_{bn}$ of the charged big grains (see Eq. (B3)), at least for input parameters not strongly different from our standard ones. Assuming now, for simplicity, that increase of $-\delta Q_s$ increases Z_b but does not affect the particle number densities n_i, n_e, n_{sk}, the absolute value of the current $e\,n_b\,Z_b\,g/\nu_{bn}$ is increased but simultaneously τ_E is decreased according to Eq. (A4). If n_i, n_e, n_{sk} dominate the electrical conductivity $1/(4\pi\,\tau_E)$ of the medium rather than the charged big grains then the electric field increases with increasing Z_b. In contrast, for large charge numbers Z_b for which $1/(4\pi\,\tau_E)$ becomes dominated by the charged big grains we have $1/(4\pi\,\tau_E) \sim Z_b^2$ (see Eq. (A4)) resulting in a decrease of the electric field with increasing Z_b as described by Eq. (B5). In fact, as mentioned above, also the absolute value of the average charge q_s carried away by the small grains may become larger if $-\delta Q_s$ is increased, so that the contribution of the charged small grains to the electrical conductivity increases, leading to a decrease of τ_E in addition to that caused by the increase of Z_b. This tends to reduce the peak electric field. We find from numerical calculations for the standard 1 A.U. parameters, but varying δQ_s, that the maximum value of $E(z)$ obtained is largest when δQ_s has approximately its standard value.

Similar results are found from numerical calculations for input parameters (excepting δQ_s) at the standard 5 A.U. values, as well as the standard values for the dust enriched subdisk. The corresponding peak electric field shown in Figs. 5 and 6, respectively, is near or only slightly below the maximum possible.

Analogous results are derived if the radius a_s for the small dust grains is varied and all other input parameters have their standard values for the respective models. For a_s having a value larger than its standard value the increase of Z_b with distance z is lower and Z_b reaches a smaller value for local equilibrium at large distances (where $Z_b \sim a_s^{-1}$) if non-inductive charge transfer processes dominate charging of big grains (see Eqs. (A13), (A15), and (A16)). Then, the absolute value of the current $e\,n_b\,Z_b\,g/\nu_{bn}$ is decreased. Simultaneously, increase of a_s results in a decrease of the mobility of small grains due to $m_s\,\nu_{sn} \sim a_s^2$ which tends to reduce the contribution of charged small grains to the electrical conductivity of the medium. Also the contribution of the charged big grains to the electrical conductivity is reduced if Z_b is reduced. On the other hand, increase of a_s reduces the surface area per unit mass and thus the absorption of free electrons and ions. As a consequence n_i and n_e increase, raising the contribution of gas phase ions and electrons to the electrical conductivity. Numerical results show that for the standard 1 A.U. parameters (except a_s which is varied) the peak electric field increases from 4.7 Volts$/\lambda_{en}$ for the standard value $a_s = 10^{-5}$ cm to about twice of this value for $a_s = 5 \times 10^{-5}$ cm (compare Figs. 1 and 3) mainly due to the decrease of the mobility of small grains and to the decrease of the charge on the big grains. As a_s is increased further, up to 10^{-4}cm, the peak electric field decreases to a value an order of magnitude smaller than that for the standard case. This is mainly due to the strong increase of gas phase ion and electron number densities and the resultant increase in conductivity (Figures for the latter results are not shown).

Whereas variation of the input parameters δQ_s or a_s leads to similar conclusions for the electric field variation in case of local equilibrium (as shown in Figs. 2b and 2d) and for the variation of the peak electric field with respect to distance (if local equilibrium does not obtain), significant diffences arise if all input parameters but the radius a_b of big grains have their standard values and a_b is varied. In case of local equilibrium the electric field is not affected significantly if the input parameter a_b is varied within a wide range of values (see Fig. 2c). In contrast, if the medium is not in local equilibrium then several transient effects allow the build up of a peak electric field, which is significantly increased compared to the standard value, when a_b is increased. The magnitude of the current $e\,n_b\,Z_b\,g/\nu_{bn}$ increases as Z_b increases with distance z according to Eq. (A13) reaching an equilibrium value at large distances which does not significantly vary with a_b if the local equilibrium value of Z_b can be approximated by Eq. (A15). However, the time scale τ_{bs} or the length scale $\tau_{bs}\,v_n$ for the big grains to reach charge equilibrium decreases with increasing value for a_b as $\sim a_b^{-1}$ (see (A16)), so that the magnitude of the current $e\,n_b\,Z_b\,g/\nu_{bn}$ of charged big grains increases faster with distance z towards its equilibrium value if a_b is increased. On the other hand, small grains tend to gain less charge q_s in collisions with big grains if Z_b is nearer to the approximate equilibrium value given by (A15) (see Eqs. (18) and (A15)), contributing less to the electrical conductivity of the medium. Also charged big grains may contribute less to the electrical conductivity if a_b is increased. In fact, nu-

merical calculations which we performed (but for which we do not show figures in this paper) give a peak electric field that is 22.5 Volts$/\lambda_{\rm en}$, 8.8 Volts$/\lambda_{\rm en}$, and 5.7 Volts$/\lambda_{\rm en}$, if all input parameters but $a_{\rm b}$ have their standard 1 A.U., standard 5 A.U. and standard dust enriched subdisk values, respectively, and $a_{\rm b}$ = 1 cm. (These values are to be compared with the peak electric field strengths of 4.7 Volts$/\lambda_{\rm en}$, 1 Volt$/\lambda_{\rm en}$, and 1 Volt$/\lambda_{\rm en}$ for corresponding standard values shown by the upper curve in Fig. 1 and by the curves in Figs. 5 and 6, respectively.) If big grains are the precursors of chondrules then we expect the mass $m_{\rm b}$ to be about 10^{-2} g implying $a_{\rm b}$ to be of the order of 10^{-1} cm if $\rho_{\rm sp,b}$ has about its standard value of 1 g cm^{-3}. Nevertheless, the calculations do indicate that the electric field may have been significantly larger than derived from our standard parameters if a non-negligible fraction of big grains with $a_{\rm b}$ = 1 cm were present in addition to the precursors of chondrules.

If all input parameters but $a_{\rm b}$ and $\rho_{\rm sp,b}$ have their standard values and $a_{\rm b}$ and $\rho_{\rm sp,b}$ are varied simultaneously such that $m_{\rm b}$ is always $(4\pi/3)\times 10^{-3}$g then $\tau_{\rm bs}$ and $\tau_{\rm bs}\, v_{\rm n}$ increase with $a_{\rm b}$ as $\sim a_{\rm b}^2$ (see Eq. (A16)) resulting in transient effects with respect to grain charging which are opposite to those occurring if all input parameters have their standard values but only $a_{\rm b}$ is varied. This results in a peak electric field being smaller than that observed for our standard values although the electric field shows only a slight dependence on $\rho_{\rm sp,b}$ in case of local equilibrium as can be seen from Fig. 4.

We may use the timescales required for the establishment of an electric field strong enough to induce discharge to consider whether discharge might have been sufficiently frequent to have affected a significant amount of material in the protosolar nebula as required by the ubiquity of chondrules (e.g. Morfill et al. 1993). A rough estimate of the maximum possible fraction of the volume of a region in which the electric field is at breakdown strength, $E_{\rm Br}$, that can be heated sufficiently to melt meteoritic material is

$$f_{\rm m} \approx \frac{E_{\rm Br}^2}{8\pi\, n_{\rm n}\, H_{\rm m}} \approx 7\times 10^{-11}\left(\frac{e\,E_{\rm Br}\,\lambda_{\rm en}}{1\,{\rm eV}}\right)^2\left(\frac{n_{\rm n}}{10^{14}{\rm cm}^{-3}}\right)\left(\frac{H_{\rm m}}{\frac{5}{2}\,k_B\,T_{\rm m}}\right)^{-1} \quad (22)$$

where $H_{\rm m}$ is the energy released per molecule in the discharge channel required for chondrule formation, k_B is Boltzmann's constant and $T_{\rm m}$ = 1800K. The amount of time required for lightning to heat a substantial fraction of the volume in any region in the disk to the degree required for chondrule formation would be $f_{\rm m}^{-1}$ times the timescale to build the field up to breakdown strength, $\tau_{\rm Br}$. The requirement that this time was comparable to or less than the lifetime of the protosolar nebula, $\tau_{\rm PSN}$, gives that

$$\tau_{\rm Br} \;\le\; 7\times 10^3{\rm s}\left(\frac{e\,E_{\rm Br}\,\lambda_{\rm en}}{1\,{\rm eV}}\right)^2\left(\frac{n_{\rm n}}{10^{14}{\rm cm}^{-3}}\right) \times\left(\frac{H_{\rm m}}{\frac{5}{2}\,k_B\,T_{\rm m}}\right)^{-1}\left(\frac{\tau_{\rm PSN}}{3\times 10^6{\rm y}}\right) \quad (23)$$

A discharge event does not alter the flow or charge distribution throughout very much of the storage volume from which the discharge draws electric energy; hence, once flow and charge structures are set up in a storage volume, discharge should repeatedly reoccur at intervals of about $\tau_{\rm E}$ as defined in Appendix A.

For a model of lightning strokes where only a small fraction of neutrals is ionized within the discharge channel and where the total energy released by lightning heats gas and dust to the same temperature within the channel the energy $H_{\rm m}$ must be about $(5/2)\,k_B\,T_{\rm m}$ or larger. Much higher values for $H_{\rm m}$ result from assumptions by Horanyi et al. (1995) who performed model calculations for the expansion, cooling and recombination of an initially fully ionized discharge channel and for the energy flux reaching the surface of an embedded dust grain and its subsequent heating. They found that short duration melting and rapid cooling of dust particles can occur in lightning discharges if lightning occurs in the solar nebula where $n_{\rm n} = 10^{14}\,{\rm cm}^{-3}$ and $T_{\rm n} = 10^2$ K for the medium not affected by lightning and with $n_{\rm i} = n_{\rm e} = 10^{14}\,{\rm cm}^{-3}$, $k_B\,T_{\rm e}$ ranging from 15 eV to 60 eV but $T_{\rm i} = 10^2$ K for the initial state of the fully ionized medium within the discharge channel. Taking into account a dissociation energy of 4.5 eV for the H_2 molecules, an ionization energy of 13.6 eV for the H atoms and requiring $k_B\,T_{\rm e} \approx 15$ eV to 60 eV, the energy $H_{\rm m}$ released per molecule ranges from 47 eV to 92 eV. These values are two orders of magnitude larger than $(5/2)\,k_B\,T_{\rm m} = 0.4$ eV. On the other hand, solid material may also be molten by radiation pulses such as considered by Eisenhour & Buseck (1995) where radiation may be produced by lightning and may be predominantly absorbed by dust grains within and in the neighbourhood of lightning strokes. In this case the energy input $H_{\rm m}$ per molecule necessary to melt dust particles may be even smaller than $(5/2)\,k_B\,T_{\rm m}$ if the solid mass contains only a small fraction of the total mass. Thus the value for $H_{\rm m}$ is rather uncertain.

The upper curve in Fig. 1 shows a maximum of $E = E_{\rm Max} \approx 4.7\,{\rm Volts}/\lambda_{\rm en}$ at $z = z_{\rm Max} = 4\times 10^9$ cm, and then a slow decay of E with increasing z where the electric field reaches half of its maximum value at $z = z_{\rm Half} = 5.2\times 10^{10}$ cm. The time scale $\tau_{\rm E}$ as defined by (A4) was numerically determined to be $\tau_{\rm E} = \tau_{\rm E,Max} \approx 7.7\times 10^4$ s at $z = z_{\rm Max}$ and $\tau_{\rm E} = \tau_{\rm E,Half} \approx 1.6\times 10^4$ s at $z = z_{\rm Half}$. According to condition (23) the time scale $\tau_{\rm Br}$ to build up the electric field up to break down field strength $E_{\rm Br}$ should be smaller than 1.6×10^5 s $(5/2)\,k_B\,T_{\rm m}\,H_{\rm m}^{-1}$ if we set $E_{\rm Br} = E_{\rm Max}$ and smaller than 4×10^4 s $(5/2)\,k_B\,T_{\rm m}\,H_{\rm m}^{-1}$ if we set $E_{\rm Br} = E_{\rm Max}/2$. Thus, we see from $\tau_{\rm Br} = \tau_{\rm E}$ that if lightning were to occur as described in this paper, then condition (23) should have been satisfied for our standard 1 A.U. parameters given in Table 1 if $H_{\rm m}$ is not significantly larger than $(5/2)\,k_B\,T_{\rm m}$. In case of $H_{\rm m} \ge 50$ eV as resulting from the assumptions by Horanyi et al. (1995) only one percent or less of the volume where the electric field is built up to break down strength is sufficiently heated.

Pilipp et al. (1992) derived an estimate for the lower limit of the lengthscale L of a region in which the electric field is strong enough to induce lightning if lightning could give rise to sufficient heating in the discharge channels for melting chondrules.

According to their arguments the maximum energy released per molecule in the discharge channel during discharge is given by

$$H_{\rm Max} \approx \frac{E_{\rm Br}^2 L^3/(8\pi)}{L w^2 n_{\rm n}} \quad (24)$$

where w is the width of the lightning bolt and where the length of the lightning bolt is assumed to be L. Since the thickness of a lightning bolt in the Earth's atmosphere is typically few thousand electron mean free paths Pilipp et al. assumed that also the width w of a discharge channel in the protosolar nebula is of the same magnitude, i.e. 5000 $\lambda_{\rm en}$, if the lightning bolt has reached a length larger than $(5000)^2\,\lambda_{\rm en}$. Here, we use a similar estimate for the value of w. Requiring that $H_{\rm Max} \geq H_{\rm m}$ we get from (24)

$$L \geq 1.2\times 10^{10}\,{\rm cm}\left(\frac{e\,E_{\rm Br}\,\lambda_{\rm en}}{1\,{\rm eV}}\right)^{-1}\left(\frac{n_{\rm n}}{10^{14}{\rm cm}^{-3}}\right)^{-3/2} \times\left(\frac{w}{10^4\,\lambda_{\rm en}}\right)\left(\frac{H_{\rm m}}{\frac{5}{2}\,k_B\,T_{\rm m}}\right)^{1/2} \quad (25)$$

Condition (25) yields $L \geq 5.1\times 10^9$ cm if we set $E_{\rm Br} = E_{\rm Max}/2$ and $w = 10^4\lambda_{\rm en} = 1\,{\rm km}\,(n_{\rm n}/(10^{14}\,{\rm cm}^{-3}))^{-1}$. From $L = z_{\rm Half} - z_{\rm Max} = 4.8\times 10^{10}$ cm we see that in this case also condition (25) is satisfied for $H_{\rm m} \leq 10^2\,((5/2)\,k_B\,T_{\rm m}) \approx 40\,{\rm eV}$.

Note that the distance $z_{\rm Half} - z_{\rm Max}$ as derived from our stationary model depends on the bulk velocity $v_{\rm n}$ which in case of our standard 1 A.U. parameters is about 5% of the sound velocity $c_{\rm sound}$. Since the time scales for the variation of the electric field should not significantly depend on the turbulent gas velocity $v_{\rm n}$ (see also Appendix A for relevant time scales) and since the time scales are converted to appropriate length scales by multiplication with $v_{\rm n}$ for the electric field we expect that the distance $L = z_{\rm Half} - z_{\rm Max}$ varies approximately as $\sim v_{\rm n}$. That is, for $H_{\rm m}$ not significantly larger than $(5/2)\,k_B\,T_{\rm m} = 0.4\,{\rm eV}$ condition (25) is satisfied already for moderate turbulent velocities $v_{\rm n} \approx 5\times 10^{-3}\,c_{\rm sound}$, whereas for the large turbulent velocities assumed by our standard parameters condition (25) is fulfilled even if $H_{\rm m}$ is as large as 40 eV.

Similar conclusions can be drawn from Fig. 3 and corresponding time scales $\tau_{\rm E}$. Here, condition (23) is again fairly well fulfilled and condition (25) is fulfilled probably for even lower turbulent velocities $v_{\rm n}$ than in case of the upper curve in Fig. 1 if $H_{\rm m} = (5/2)\,k_B\,T_{\rm m}$ is assumed.

As mentioned above, numerical calculations performed by us (but for which figures are not shown) for which all input parameters but $a_{\rm b}$ have the standard 1 A.U. values and $a_{\rm b} = 1$ cm, give a maximum electric field $E_{\rm Max} = 22.5\,{\rm Volts}/\lambda_{\rm en}$ with respect to variation with distance z. In this case, conditions (23) and (25) are fulfilled for even higher values of $H_{\rm m}$ and/or probably lower turbulent gas velocities. On the other hand, we find from curves shown in Fig. 4a and corresponding time scales $\tau_{\rm E}$ that the maximum electric field $E_{\rm Max}$ decreases with decreasing specific mass density $\rho_{\rm sp,b}$ but constant mass $m_{\rm b}$ for the big grains and that conditions (23) and (25) can be fulfilled only if $H_{\rm m}$ decreases with decreasing value for $\rho_{\rm sp,b}$.

For Fig. 5, the maximum of the electric field strength of about $E = E_{\rm Max} \approx 1\,{\rm Volt}/\lambda_{\rm en}$ occurs at $z = z_{\rm Max} = 2.7\times 10^{10}$ cm, and the electric field strength decays to $E_{\rm Half} = E_{\rm Max}/2$ at $z = z_{\rm Half} = 3.1\times 10^{11}$ cm. The time scale $\tau_{\rm E}$ was determined to be $\tau_{\rm E} = \tau_{\rm E,Max} \approx 2.3\times 10^4$ s at $z = z_{\rm Max}$ and $\tau_{\rm E} = \tau_{\rm E,Half} \approx 4\times 10^3$ s at $z = z_{\rm Half}$. For $n_{\rm n} = 10^{13}\,{\rm cm}^{-3}$ as is the case for our standard 5 A.U. parameters, condition (23) yields $\tau_{\rm Br} \leq 7\times 10^2\,{\rm s}\,(5/2)\,k_B\,T_{\rm m}\,H_{\rm m}^{-1}$ if we set $E_{\rm Br} = E_{\rm Max}$ and $\tau_{\rm Br} \leq 1.8\times 10^2\,{\rm s}\,(5/2)\,k_B\,T_{\rm m}\,H_{\rm m}^{-1}$ if we set $E_{\rm Br} = E_{\rm Max}/2$. That is, from $\tau_{\rm Br} = \tau_{\rm E}$ condition (23) fails by an order of magnitude for $H_{\rm m} \approx (5/2)\,k_B\,T_{\rm m}$. Condition (25) requires $L \geq 8\times 10^{11}\,{\rm cm}\,H_{\rm m}^{1/2}\,((5/2)\,k_B\,T_{\rm m})^{-1/2}$ for $E_{\rm Br} = E_{\rm Max}/2$ and $w = 10^4\,\lambda_{en} = 10\,{\rm km}\,(n_{\rm n}/(10^{13}\,{\rm cm}^{-3}))^{-1}$ which is barely fulfilled for $L = z_{\rm Half} - z_{\rm Max} = 2.8\times 10^{11}$ cm.

From numerical calculations for which all input parameters but $a_{\rm b}$ have their standard 5 A.U. values and $a_{\rm b} = 1$ cm (mentioned above) we found that $E_{\rm Max} = 8.8\,{\rm Volts}/\lambda_{\rm en}$ and that both conditions (23) and (25) can be fulfilled if $H_{\rm m}$ is of the order of $(5/2)\,k_B\,T_{\rm m}$.

For Fig. 6, the maximum of the electric field strength of about $E = E_{\rm Max} \approx 1\,{\rm Volt}/\lambda_{\rm en}$ occurs at $z = z_{\rm Max} = 2.4\times 10^8$ cm, and the electric field strength decays to $E = E_{\rm Max}/2$ at $z = z_{\rm Half} = 3\times 10^9$ cm. The time scale $\tau_{\rm E}$ was determined to be $\tau_{\rm E} = \tau_{\rm E,Max} \approx 2.7\times 10^3$ s at $z = z_{\rm Max}$ and $\tau_{\rm E} = \tau_{\rm E,Half} \approx 2\times 10^2$ s at $z = z_{\rm Half}$. For $n_{\rm n} = 2\times 10^{13}\,{\rm cm}^{-3}$ as is the case for our standard parameters for the dust enriched subdisk condition (23) yields $\tau_{\rm Br} \leq 1.4\times 10^3\,{\rm s}\,(5/2)\,k_B\,T_{\rm m}\,H_{\rm m}^{-1}$ if we set $E_{\rm Br} = E_{\rm Max}$ and $\tau_{\rm Br} \leq 3\times 10^2\,{\rm s}\,(5/2)\,k_B\,T_{\rm m}\,H_{\rm m}^{-1}$ if we set $E_{\rm Br} = E_{\rm Max}/2$. Thus, condition (23) should be fulfilled at least if $H_{\rm m}$ is not significantly larger than $(5/2)\,k_B\,T_{\rm m}$. However, condition (25) requiring $L \geq 2\times 10^{11}\,{\rm cm}\,H_{\rm m}^{1/2}\,((5/2)\,k_B\,T_{\rm m})^{-1/2}$ for $E_{\rm Br} = E_{\rm Max}/2$ and for $w = 10^4\,\lambda_{\rm en}$ fails by two orders of magnitude for $H_{\rm m} \geq (5/2)\,k_B\,T_{\rm m}$. At large distances, say at $z = 10^{11}$ cm, the electric field has decreased to about $0.23\,{\rm Volts}/\lambda_{\rm en}$, where the time scale $\tau_{\rm E}$ was determined to be $\tau_{\rm E} \approx 4\times 10^1$ s and where conditions (23) and (25) require $\tau_{\rm Br} \leq 7\times 10^1\,{\rm s}\,(5/2)\,k_B\,T_{\rm m}\,H_{\rm m}^{-1}$ and $L \geq 5\times 10^{11}\,{\rm cm}\,H_{\rm m}^{1/2}\,((5/2)\,k_B\,T_{\rm m})^{-1/2}$ respectively. Again, condition (23) is fairly well fulfilled whereas condition (25) fails at least by a factor 5 for $H_{\rm m} \geq (5/2)\,k_B\,T_{\rm m}$.

From numerical calculations for which all input parameters but $a_{\rm b}$ have their standard values for the dust enriched subdisk and $a_{\rm b} = 1$ cm (mentioned above) we found that $E_{\rm Max} = 5.7\,{\rm Volts}/\lambda_{\rm en}$ and that condition (23) can easily be fulfilled for $H_{\rm m} \leq 10\times(5/2)\,k_B\,T_{\rm m}$. Condition (25) fails by more than an order of magnitude if $H_{\rm m} \geq (5/2)\,k_B\,T_{\rm m}$ and if the lenth $z_{\rm Half} - z_{\rm Max}$ between the position $z = z_{\rm Max}$ where the electric field reaches its peak value and the position $z = z_{\rm Half}$ beyond $z = z_{\rm Max}$ where the electric field has decreased to half of its peak value is compared with the right hand side of relation (25). However, if the distance range $z_1 - z_{\rm Half}$ from position $z = z_{\rm Half}$ where $E = E_{\rm Max}/2 = 2.84\,{\rm Volts}/\lambda_{\rm en}$ and position $z = z_1$ beyond $z = z_{\rm Half}$ where the electric field has decreased to $1\,{\rm Volt}/\lambda_{\rm en}$ is compared with the right hand side of relation (25) then condition (25) is fairly well fulfilled for $H_{\rm m} \approx (\frac{5}{2}\,k_B\,T_{\rm m})$.

6. Conclusions

We conclude that lightning capable of melting a significant fraction of solid material could indeed have occurred in the protosolar nebula. However, this requires some special conditions, which we briefly summarize.

1. We found that global electric fields strong enough to induce lightning could have been generated only if charge transfer processes operated in grain-grain collisions, which were much more effective than grain charging by the Elster-Geitel mechanism and by impact of gas phase ions and electrons on the grains.

2. The gas phase ionization rate has to be much lower than that usually assumed for molecular clouds and is required to be almost as low as that resulting from decay of long-lived radioactive elements trapped in the grains alone. Cosmic ray ionization has to be at most of this same magnitude.

3. Generation of strong electric fields is more likely if local ionization equilibrium did not obtain.

4. Strong electric fields can be generated more easily if precursors of chondrules were compact with a specific mass density not much lower that $1\,\mathrm{g\,cm^{-3}}$. This condition does not necessarily mean that all precursors of chondrules had to be compact but at least a significant fraction of the mm to cm sized grains had to be sufficiently compact in addition to fluffy precursors of the chondrules.

5. For our models corresponding to the protosolar nebula near 1 A.U. the energy released in lightning strokes was found to be large enough to melt solid material. One possibility is that the solid material within a discharge channel melts, if the gas is heated up to the melting temperature of 1800 K (i.e. $H_\mathrm{m} = (5/2)\,k_B\,T_\mathrm{m}$) and the turbulent gas velocity is at least 0.5 per cent of the sound velocity. Another possibility is that the energy H_m released in a lightning stroke is 40 eV per H_2 molecule (in accordance with assumptions by Horanyi et al. (1995)) and the turbulent gas velocity is as large as assumed by our standard parameters.

6. For our models corresponding to 5 A.U. lightning strokes capable of melting chondrules were found e.g. under the assumption that $H_\mathrm{m} = (5/2)\,k_B\,T_\mathrm{m}$ and the turbulent gas velocity was at least of the order of 10 per cent of the sound velocity.

7. For the dust enriched subdisk we found that for our standard parameters and assuming $H_\mathrm{m} = (5/2)\,k_B\,T_\mathrm{m}$, the energy released in a lightning stroke was much too low to melt chondrules. Our results indicate that chondrules might have been molten here also in lightning discharges, provided a significant fraction of big grains were cm sized massive particles with a specific density of $1\,\mathrm{g\,cm^{-3}}$.

8. If a much lower energy release within the lightning channel was sufficient to melt solid material as could be inferred from the work of Eisenhour & Buseck (1995), then the requirements are less stringent than those mentioned in 5 -7.

9. The occurrence frequency of lightning discharges was found to be large enough to affect a significant amount of material in the protosolar nebula for our models near 1 A.U. and for the dust enriched subdisk if $H_\mathrm{m} \leq (5/2)\,k_B\,T_\mathrm{m}$.

10. For our models at 5 A.U. and for corresponding standard parameters only few per cent of the material in the nebula was affected during its lifetime if $H_\mathrm{m} = (5/2)\,k_B\,T_\mathrm{m}$ is assumed. However, our calculations indicate that here, too, a large fraction of the volume of the nebula might have been heated sufficiently to melt chondrules if a significant fraction of dust consisted of cm sized grains with a specific mass density of order unity.

In the present paper we left out questions concerning time scales for heating and cooling of chondrules and their precursors, respectively, and size distributions of chondrules as expected from flash-heating by lightning discharges and their comparison with petrologic limits. Such questions have been treated by Horanyi et al. (1995) and in context with heating by radiation pulses by Eisenhour & Buseck (1995).

The identification of a sufficiently effective process for charge transfer between grains and a more rigorous justification of the assumption of a low gas phase ionization rate remain as the primary problems in the production of lightning in the protosolar nebula.

Acknowledgements. We thank S.G. Love for careful review of this paper and useful comments.

Appendix A: the timescales for the generation of the electric field and for the attainment of ionization equilibrium

We define

$$Q \equiv n_\mathrm{i} - n_\mathrm{e} + n_\mathrm{b}\,Z_\mathrm{b} + \sum_k n_{sk}\,k \tag{A1}$$

so that Eq. (10) is

$$\frac{\mathrm{d}E}{\mathrm{d}z} = 4\pi e\,Q \tag{A2}$$

Using (20b) and Eqs. (6) through (9) we find

$$Q = \frac{1}{4\pi e\,v_\mathrm{n}}\left[-\frac{E}{\tau_\mathrm{E}} + 4\pi J - 4\pi e\left(n_\mathrm{b}\,Z_\mathrm{b}\,\frac{g}{\nu_\mathrm{bn}} + \sum_k n_{sk}\,k\,\frac{g}{\nu_\mathrm{sn}}\right)\right] \tag{A3}$$

with

$$\tau_\mathrm{E} \equiv \left[4\pi e^2\left(\frac{n_\mathrm{i}}{m_\mathrm{i}\,\nu_\mathrm{in}} + \frac{n_\mathrm{e}}{m_\mathrm{e}\,\nu_\mathrm{en}} + \frac{n_\mathrm{b}\,Z_\mathrm{b}^2}{m_\mathrm{b}\,\nu_\mathrm{bn}} + \sum_k \frac{n_{sk}\,k^2}{m_\mathrm{s}\,\nu_\mathrm{sn}}\right)\right]^{-1} \tag{A4}$$

Clearly, in the absence of charged grains the e - folding growth timescale τ_E of the electric field would be given by

$$\tau_\mathrm{E0} \equiv \left[4\pi e^2\left(\frac{n_\mathrm{i}}{m_\mathrm{i}\,\nu_\mathrm{in}} + \frac{n_\mathrm{e}}{m_\mathrm{e}\,\nu_\mathrm{en}}\right)\right]^{-1} \tag{A5}$$

We also define

$$\tau_\mathrm{Eb} \equiv \left(4\pi e^2\,\frac{n_\mathrm{b}\,Z_\mathrm{b}^2}{m_\mathrm{b}\,\nu_\mathrm{bn}}\right)^{-1} \tag{A6}$$

and

$$\tau_{\rm Es} \equiv \left(4\pi e^2 \sum_k n_{sk}\, k^2\, \frac{1}{m_{\rm s}\, \nu_{\rm sn}} \right)^{-1} \tag{A7}$$

Then from (A4) to (A7)

$$\tau_{\rm E} = \left(\frac{1}{\tau_{\rm E0}} + \frac{1}{\tau_{\rm Eb}} + \frac{1}{\tau_{\rm Es}} \right)^{-1} \tag{A8}$$

and each of $\tau_{\rm E0}$, $\tau_{\rm Eb}$, and $\tau_{\rm Es}$ is an upper bound to $\tau_{\rm E}$.

The following estimates are based on various conditions which are discussed in Appendix C.

To estimate $\tau_{\rm E0}$, $\tau_{\rm Eb}$, and $\tau_{\rm Es}$ we must estimate $n_{\rm i}$, $n_{\rm e}$, $Z_{\rm b}$, and n_{sk}. We find from (1) and (2b) and evaluations of Γ's that to a good approximation for cases that we have studied

$$n_{\rm i} \approx \frac{\zeta\, n_{\rm n}}{\Gamma_{\rm is0}\, n_{\rm s}} \tag{A9}$$

and

$$n_{\rm e} \approx \frac{\zeta\, n_{\rm n}}{-(\Gamma_{\rm eb}\, n_{\rm b} + \Gamma_{\rm es0}\, n_{\rm s})} \tag{A10}$$

and that the timescale for $n_{\rm i}$ and $n_{\rm e}$ to reach local steady state equilibrium values are less than about

$$\begin{aligned} \tau_{\rm i} &\equiv \frac{1}{\Gamma_{\rm is0}\, n_{\rm s}} \\ &\approx 1\times 10^2{\rm s} \left(\frac{a_{\rm s}}{1\times 10^{-5}{\rm cm}} \right) \left(\frac{\rho_{\rm sp,s}}{1\,{\rm g\,cm^{-3}}} \right) \\ &\quad \times \left(\frac{T_{\rm n}}{750\,{\rm K}} \right)^{-1/2} \left(\frac{\rho_{\rm s}/\rho_{\rm n}}{5\times 10^{-3}} \right)^{-1} \left(\frac{n_{\rm n}}{10^{14}\,{\rm cm^{-3}}} \right)^{-1} \end{aligned} \tag{A11}$$

$$\tau_{\rm e} \equiv \frac{1}{-\Gamma_{\rm es0}\, n_{\rm s}} \approx 5\times 10^{-3} \tau_{\rm i} \tag{A12}$$

respectively. $\rho_{\rm sp,s}$ and $\rho_{\rm sp,b}$ are the average specific mass densities inside the small and big grains.

From Eqs. (4), (5), (15), and assuming $v_{\rm b} < v_{sk}$ as done to derive (15), we find

$$\begin{aligned} v_{\rm b} \frac{{\rm d}Z_{\rm b}}{{\rm d}z} &= -\frac{Z_{\rm b}}{\tau_{\rm bs}} - \left(\frac{\delta Q_{\rm s}\, a_{\rm s}}{e} \right) \left(\frac{4\pi a_{\rm b}^2}{\gamma \pi a_{\rm s}^2} \right) \frac{1}{\tau_{\rm bs}} \\ &\quad + \frac{E}{2\pi e} \frac{4\pi a_{\rm b}^2}{\tau_{\rm bs}} + \sum_k k\, n_{sk}\, (v_{sk} - v_{\rm b})\, \pi a_{\rm b}^2 \\ &\quad + \Gamma_{\rm ib}\, n_{\rm i} + \Gamma_{\rm eb}\, n_{\rm e} \end{aligned} \tag{A13}$$

with

$$\tau_{\rm bs} \equiv \frac{4}{\sum_k n_{sk}\, (v_{sk} - v_{\rm b})\, \gamma \pi a_{\rm s}^2} \tag{A14}$$

Taking only the first and second term on the right hand side of Eq. (A13) into account and neglecting all the other terms, we get in the case of local equilibrium

$$Z_{\rm b} \approx -\left(\frac{\delta Q_{\rm s}\, a_{\rm s}}{e} \right) \left(\frac{4\pi a_{\rm b}^2}{\gamma \pi a_{\rm s}^2} \right) \tag{A15}$$

In fact, as will be discussed in more detail in Appendix C, (A15) is a good approximation for our 1 A.U. standard parameters and standard parameters for the dust enriched subdisk. For our 5 A.U. standard parameters the term $\Gamma_{\rm eb}\, n_{\rm e}$ may be a significant fraction of the term $-(\delta Q_{\rm s}\, a_{\rm s}/e)\, (4\pi a_{\rm b}^2/\gamma \pi a_{\rm s}^2)\, (1/\tau_{\rm bs})$ decreasing $Z_{\rm b}$ signicantly as compared to approximation (A15), but even in this case (A15) can still be considered to be an order of magnitude estimate.

Approximating $v_{sk} - v_{\rm b} \approx v_{\rm n} - v_{\rm b} > 0$ and estimating $v_{\rm n} - v_{\rm b}$ from Eq. (8) with $Z_{\rm b}\, e\, E \ll m_{\rm b} \mid g \mid$ we find

$$\begin{aligned} \tau_{\rm bs} &\approx 6\times 10^5{\rm s} \left(\frac{1}{\gamma} \right) \\ &\quad \times \left(\frac{T_{\rm n}}{750{\rm K}} \right)^{1/2} \left(\frac{a_{\rm s}}{1\times 10^{-5}{\rm cm}} \right) \left(\frac{\rho_{\rm sp,s}}{1\,{\rm g\,cm^{-3}}} \right) \\ &\quad \times \left(\frac{\rho_{\rm s}/\rho_{\rm n}}{5\times 10^{-3}} \right)^{-1} \left(\frac{g}{-5\times 10^{-2}{\rm cm\,s^{-2}}} \right)^{-1} \\ &\quad \times \left(\frac{a_{\rm b}}{1\times 10^{-1}{\rm cm}} \right)^{-1} \left(\frac{\rho_{\rm sp,b}}{1\,{\rm g\,cm^{-3}}} \right)^{-1} \end{aligned} \tag{A16}$$

From (3) and the evaluations of the Γ's and ν's we see that for cases in which parameters differ little from the standard ones once equilibrium is reached

$$\sum_k n_{sk}\, k^2 \approx n_{\rm s1} + n_{\rm s\,-1} \approx \frac{2\,\zeta\, n_{\rm n}}{\pi a_{\rm b}^2\, n_{\rm b}\, (v_{\rm n} - v_{\rm b})} \tag{A17}$$

and small grains carrying charges with a magnitude larger than one elementary charge can be neglected. Approximation (A17) is a good approximation for our 1 A.U. standard parameters and for our standard parameters for the dust enriched subdisk. For our 5 A.U. standard parameters (A17) is less accurate but still an order of magnitude estimate. The local equilibrium distribution of small grain charges is reached on a timescale of

$$\begin{aligned} \tau_{\rm sb} &= \frac{1}{\pi a_{\rm b}^2\, n_{\rm b}\, (v_{\rm n} - v_{\rm b})} \\ &\approx 1.5\times 10^9{\rm s} \left(\frac{T_{\rm n}}{750\,{\rm K}} \right)^{1/2} \\ &\quad \times \left(\frac{g}{-5\times 10^{-2}\,{\rm cm\,s^{-2}}} \right)^{-1} \left(\frac{\rho_{\rm b}/\rho_{\rm n}}{5\times 10^{-3}} \right)^{-1} \end{aligned} \tag{A18}$$

With the use of the local equilibrium values of $n_{\rm i}$, $n_{\rm e}$, $Z_{\rm b}$, $n_{\rm s\,-1}$, and $n_{\rm s1}$ and expressions for $\nu_{\rm in}, \nu_{\rm en}, \nu_{\rm bn}$, and $\nu_{\rm sn}$ evaluated under the assumption that the motions of the dust grains relative to the neutrals are very subthermal we obtain the following approximations which are reliable for parameters near the standard ones.

$$\begin{aligned} \tau_{\rm E0} &\approx 2\times 10^5{\rm s} \\ &\quad \times \left(\frac{\rho_{\rm s}/\rho_{\rm n}}{5\times 10^{-3}} \right) \left(\frac{n_{\rm n}}{10^{14}\,{\rm cm^{-3}}} \right) \\ &\quad \times \left(\frac{\zeta}{10^{-22}\,{\rm s^{-1}}} \right)^{-1} \left(\frac{a_{\rm s}}{1\times 10^{-5}{\rm cm}} \right)^{-1} \\ &\quad \times \left(\frac{\rho_{\rm sp,s}}{1\,{\rm g\,cm^{-3}}} \right)^{-1} A^{-1} \end{aligned} \tag{A19}$$

where A is about 0.3 when $E \approx 1\mathrm{V}/\lambda_{\mathrm{en}}$ and $T_{\mathrm{e}} = 10^4$ K and becomes larger for E and T_{e} becoming smaller.

$$\tau_{\mathrm{Eb}} \approx 2 \times 10^4 \mathrm{s}\, \gamma^2 \left(\frac{a_{\mathrm{b}}}{1 \times 10^{-1}\mathrm{cm}}\right) \times \left(\frac{\rho_{\mathrm{sp,b}}}{1\mathrm{g\,cm}^{-3}}\right) \left(\frac{T_{\mathrm{n}}}{750\mathrm{K}}\right)^{1/2} \left(\frac{a_{\mathrm{s}}}{1 \times 10^{-5}\mathrm{cm}}\right)^2 \times \left(\frac{\rho_{\mathrm{b}}/\rho_{\mathrm{n}}}{5 \times 10^{-3}}\right)^{-1} \left(\frac{\delta Q_{\mathrm{s}}}{-1.44 \times 10^{-2}\,\mathrm{V}}\right)^{-2} \quad \text{(A20)}$$

and

$$\tau_{\mathrm{Es}} \approx 4.5 \times 10^2 \mathrm{s} \times \left(\frac{a_{\mathrm{s}}}{1 \times 10^{-5}\,\mathrm{cm}}\right)^2 \left(\frac{g}{-5 \times 10^{-2}\mathrm{cm\,s}^{-2}}\right) \times \left(\frac{\rho_{\mathrm{b}}/\rho_{\mathrm{n}}}{5 \times 10^{-3}}\right) \left(\frac{\zeta}{1 \times 10^{-22}\,\mathrm{s}^{-1}}\right)^{-1} \quad \text{(A21)}$$

Conditions on which approximations (A19) to (A21) are based are discussed in more detail in Appendix C. These conditions are fulfilled only if local charge equilibrium prevails. The timescale τ_{E0}, being an upper bound to τ_{E}, can be approximated by (A19) if the gas phase ions and electrons have reached local equilibrium for their number densities even if the grains are not in local charge equilibrium. This condition should be fulfilled if the amount of time which has passed during the evolution of a dynamic structure is large compared to τ_{i} as defined and approximated by (A11), or in our stationary models, for lengthscales z large compared to $\tau_{\mathrm{i}}\, v_{\mathrm{i}}$ with $v_{\mathrm{i}} \approx 2.5 \times 10^5\,\mathrm{cm\,s}^{-1}\,(E/(\mathrm{V}/\lambda_{\mathrm{en}})) + v_{\mathrm{n}}$. (For electrons we have used the approximation of local equilibrium anyway, i.e. Eq. (2b) in place of (2a)). Analogously, the timescale τ_{Eb}, being an upper bound to τ_{E}, can be approximated by (A20) if the big grains have reached local charge equilibrium even if the small grains are not in local charge equilibrium. This condition should be fulfilled for lengthscales z large compared to $\tau_{\mathrm{bs}}\, v_{\mathrm{n}}$. Finally, the timescale τ_{Es} can be approximated by (A21) only if the small grains have reached local charge equilibrium, which should occur only at distances large compared to $\tau_{\mathrm{sb}}\, v_{\mathrm{n}}$. In fact, because local charge equilibrium for the small grains is reached on lengthscales greater than the thickness of the protosolar nebula for many sets of parameters and because local equilibrium electric fields are usually weaker than those at which discharge is induced, the τ_{E}'s in many storage volumes capable of powering discharges that could have formed chondrules cannot be estimated by (A8) if τ_{Es} is approximated by (A21). However, approximation (A21) for the timescale τ_{Es} is useful for the interpretation of physical processes causing the variation of the local equilibrium electric field with various parameters.

Appendix B: upper bounds and the equilibrium values of the electric field

For the electric field E as a function of z we have $\mathrm{d}E/\mathrm{d}z = 0$ at the position z where E reaches a peak value, and also at sufficiently large distances z where the medium reaches local equilibrium. Taking $J = 0$, (A2) and (A3) give for these cases the electric field strength

$$E = -4\pi e \left(n_{\mathrm{b}}\, Z_{\mathrm{b}}\, \frac{g}{\nu_{\mathrm{bn}}} + \sum_k n_{\mathrm{s}k}\, k\, \frac{g}{\nu_{\mathrm{sn}}}\right) \tau_{\mathrm{E}} \quad \text{(B1)}$$

For the adopted standard values of relevant parameters grains carry far more of the charge than gas phase ions or electrons do, except for a small region near the boundary $z = 0$ in z - space. Thus, (A1) and (A2) imply that for $\mathrm{d}E/\mathrm{d}z = 0$

$$n_{\mathrm{b}}\, Z_{\mathrm{b}} \approx -\sum_k n_{\mathrm{s}k}\, k \quad \text{(B2)}$$

$\nu_{\mathrm{bn}} \ll \nu_{\mathrm{sn}}$ implies together with (B1) and (B2) that at positions where $\mathrm{d}E/\mathrm{d}z = 0$

$$E \approx -4\pi e \left(n_{\mathrm{b}}\, Z_{\mathrm{b}}\, \frac{g}{\nu_{\mathrm{bn}}}\right) \tau_{\mathrm{E}} \quad \text{(B3)}$$

In fact, (B3) holds approximately whenever $\mid \mathrm{d}E/\mathrm{d}z \mid \ll \mid E/(\tau_{\mathrm{E}}\, v_{\mathrm{n}}) \mid$ and we will use (B3) as an approximation for the electric field variation for distances $z \gg \tau_{\mathrm{E0}}\, v_{\mathrm{n}} > \tau_{\mathrm{E}}\, v_{\mathrm{n}}$. Using approximation (A19) we get $\tau_{\mathrm{E0}}\, v_{\mathrm{n}} = 2 \times 10^9 (1/A)\,\mathrm{cm}$, $4 \times 10^8 (1/A)\,\mathrm{cm}$, $2 \times 10^8 (1/A)\,\mathrm{cm}$, and $1.6 \times 10^8 (1/A)\,\mathrm{cm}$ for Figs. 1, 3, 5, and 6, respectively.

According to (A8) we have $\tau_{\mathrm{E}} < \tau_{\mathrm{Eb}}$, which yields with (B3)

$$E < E_{\mathrm{b}} \quad \text{(B4)}$$

where E_{b} is defined as

$$E_{\mathrm{b}} \equiv -4\pi e \left(n_{\mathrm{b}}\, Z_{\mathrm{b}}\, \frac{g}{\nu_{\mathrm{bn}}}\right) \tau_{\mathrm{Eb}} = -\frac{m_{\mathrm{b}}\, g}{e\, Z_{\mathrm{b}}} \quad \text{(B5)}$$

We define

$$Z_{\mathrm{b,Q}} \equiv -\left(\frac{\delta Q_{\mathrm{s}}\, a_{\mathrm{s}}}{e}\right) \left(\frac{4\pi a_{\mathrm{b}}^2}{\gamma \pi a_{\mathrm{s}}^2}\right) \quad \text{(B6)}$$

For our standard parameters we have $Z_{\mathrm{b,Q}} = 4 \times 10^8$. According to (A15) we have $Z_{\mathrm{b}} \approx Z_{\mathrm{b,Q}}$ in case of local charge equilibrium and for our standard parameters. Inserting (B6) and (B5) into (B4) yields

$$E < 3.3\,(\mathrm{V}/\lambda_{\mathrm{en}})\,\gamma \left(\frac{Z_{\mathrm{b,Q}}}{Z_{\mathrm{b}}}\right) \left(\frac{g}{-5 \times 10^{-2}\mathrm{cm\,s}^{-2}}\right) \times \left(\frac{a_{\mathrm{b}}}{10^{-1}\mathrm{cm}}\right) \left(\frac{a_{\mathrm{s}}}{10^{-5}\mathrm{cm}}\right) \left(\frac{\rho_{\mathrm{sp,b}}}{1\,\mathrm{g\,cm}^{-3}}\right) \times \left(\frac{\delta Q_{\mathrm{s}}}{-1.44 \times 10^{-2}\mathrm{V}}\right)^{-1} \left(\frac{n_{\mathrm{n}}}{10^{14}\mathrm{cm}^{-3}}\right)^{-1} \quad \text{(B7)}$$

When local equilibrium obtains, and for values of the parameters near the standard ones that we have adopted τ_{E} may be estimated by τ_{Es} as given by approximation (A21) and Z_{b} may

be estimated by (A15). Hence, (B3) yields a local equilibrium electric field strength which is roughly

$$E \approx 6.9 \times 10^{-2} \left(\frac{\mathrm{V}}{\lambda_{\mathrm{en}}}\right) \left(\frac{1}{\gamma}\right) \left(\frac{\rho_{\mathrm{b}}/\rho_{\mathrm{n}}}{5 \times 10^{-3}}\right)^2 \times \left(\frac{g}{-5 \times 10^{-2}\mathrm{cm\,s^{-2}}}\right)^2 \left(\frac{\delta Q_{\mathrm{s}}}{-1.44 \times 10^{-2}\mathrm{V}}\right) \times \left(\frac{a_{\mathrm{s}}}{10^{-5}\mathrm{cm}}\right) \left(\frac{\zeta}{10^{-22}\mathrm{s^{-1}}}\right)^{-1} \times \left(\frac{T_{\mathrm{n}}}{750\,\mathrm{K}}\right)^{-1/2} \left(\frac{n_{\mathrm{n}}}{10^{14}\mathrm{cm^{-3}}}\right)^{-1} \quad \text{(B8)}$$

(B8) holds only for a restricted range of values for the relevant parameters. For parameter values significantly different from our standard ones, τ_{E} may not be estimated by τ_{Es} but possibly better by τ_{Eb} or τ_{E0}, and conditions on which (A19) to (A21) are based may not be fulfilled. Conditions on which approximations (A19) to (A21) are based and also conditions which allow the estimation of τ_{E} by τ_{Es} are discussed in more detail in Appendix C.

Appendix C: conditions for the approximations for time scales and equilibrium values

We discuss in more detail the conditions on which approximations in Appendices A and B are based.

The motions of dust grains relative to neutrals are assumed to be very subthermal, i.e.

$$\mid v_{\mathrm{n}} - v_d \mid \ll \left(\frac{2\,k_B\,T_{\mathrm{n}}}{m_{\mathrm{n}}}\right)^{1/2} = 2.5 \times 10^5 \mathrm{cm\,s^{-1}} \left(\frac{T_{\mathrm{n}}}{750\,\mathrm{K}}\right)^{1/2} \quad \text{(C1)}$$

with d = b, sk, which is well fulfilled for our standard parameters, so that approximation

$$m_d\,\nu_{d\mathrm{n}} = \frac{4}{3}\,n_{\mathrm{n}}\,m_{\mathrm{n}} \left(\frac{8\,k_B\,T_{\mathrm{n}}}{m_{\mathrm{n}}\,\pi}\right)^{1/2} \pi a_d^2$$

for d = b, s can be used (see Draine, 1986).

For the big grains the magnitude of the electric force is assumed to be small compared to the magnitude of the gravitational force, i.e.

$$Z_{\mathrm{b}}\,e\,E \ll \mid m_{\mathrm{b}}\,g \mid \quad \text{(C2)}$$

or

$$E \ll 3.25\,(\mathrm{V}/\lambda_{\mathrm{en}}) \times \left(\frac{g}{-5 \times 10^{-2}\mathrm{cm\,s^{-2}}}\right) \left(\frac{a_{\mathrm{b}}}{10^{-1}\mathrm{cm}}\right)^3 \left(\frac{\rho_{\mathrm{sp,b}}}{1\,\mathrm{g\,cm^{-3}}}\right) \times \left(\frac{Z_{\mathrm{b}}}{4 \times 10^8}\right)^{-1} \left(\frac{n_{\mathrm{n}}}{10^{14}\mathrm{cm^{-3}}}\right)^{-1} \quad \text{(C3)}$$

so that with (8)

$$v_{\mathrm{n}} - v_{\mathrm{b}} \approx \frac{-g}{\nu_{\mathrm{bn}}} \quad \text{(C4)}$$

For our standard parameters and for a local equilibrium for which $E \leq 0.1\,\mathrm{Volts}/\lambda_{\mathrm{en}}$, condition (C3) is fairly well fulfilled. If local equilibrium does not obtain condition (C3) is still barely fulfilled for our standard parameters. We also assume

$$v_{sk} - v_{\mathrm{b}} \approx v_{\mathrm{n}} - v_{\mathrm{b}} > 0 \quad \text{for all} \quad k = 0; \pm 1; \pm 2; \ldots \quad \text{(C5)}$$

With (C2), (8), (9), and $\nu_{\mathrm{bn}}/\nu_{\mathrm{sn}} = a_{\mathrm{s}}/a_{\mathrm{b}} \ll 1$ assumption (C5) gives

$$\left|\frac{k\,e\,E}{m_{\mathrm{s}}\,\nu_{\mathrm{sn}}}\right| \ll \left|\frac{g}{\nu_{\mathrm{bn}}}\right| \quad \text{(C6)}$$

or

$$E \ll \frac{13}{k}(\mathrm{V}/\lambda_{\mathrm{en}}) \times \left(\frac{a_{\mathrm{s}}}{10^{-5}\mathrm{cm}}\right)^2 \left(\frac{a_{\mathrm{b}}}{10^{-1}\mathrm{cm}}\right) \left(\frac{\rho_{\mathrm{sp,b}}}{1\,\mathrm{g\,cm^{-3}}}\right) \times \left(\frac{g}{-5 \times 10^{-2}\mathrm{cm\,s^{-2}}}\right) \left(\frac{n_{\mathrm{n}}}{10^{14}\mathrm{cm^{-3}}}\right)^{-1} \quad \text{(C7)}$$

(C7) is fulfilled in the case of a local equilibrium for which charged dust grains with $\mid k \mid = 1$ dominate the electrical conductivity of the medium and $E \leq 0.1\,\mathrm{Volts}/\lambda_{\mathrm{en}}$. For $\mid k \mid = 1$ and $E = 1\,\mathrm{Volt}/\lambda_{\mathrm{en}}$ condition (C7) is fairly well fulfilled for our standard 1 A.U. and 5 A.U. parameters but barely fulfilled for our standard parameters for the dust enriched subdisk.

We evaluate the Γ_{jd}'s with j = i, e and d = b, sk from results given by Havnes et al. (1987). For the electrons we assume

$$\frac{m_{\mathrm{e}}\,(v_{\mathrm{e}} - v_d)^2}{2\,k_B\,T_{\mathrm{e}}} \ll 1 \quad \text{(C8a)}$$

which is equivalent with

$$\frac{m_{\mathrm{e}}\,(v_{\mathrm{e}} - v_{\mathrm{n}})^2}{2\,k_B\,T_{\mathrm{e}}} \ll 1 \quad \text{(C8b)}$$

if (C1) together with $T_{\mathrm{e}} \geq T_{\mathrm{n}}$ is fulfilled. Condition (C8b) is fulfilled for an electric field strength $E \ll 0.2\,(\mathrm{V}/\lambda_{\mathrm{en}})\,(\mathrm{T_e}/(750\,\mathrm{K}))$ as is the case for our standard parameters for an electric field strength up to $2\,\mathrm{V}/\lambda_{\mathrm{en}}$ since T_{e} grows sufficiently fast with the electric field strength up to 10^4 K.
A condition for the ions analogous to (C8b) is fulfilled for $E \ll 0.26\,(\mathrm{V}/\lambda_{\mathrm{en}})\,(\mathrm{T_n}/(750\,\mathrm{K}))^{1/2}$ for which $T_{\mathrm{i}} \approx T_{\mathrm{n}}$. This is the case for our standard parameters for local equilibrium. However, for an electric field strength relevant for inducing lightning, i.e. for $E \geq 1\,\mathrm{V}/\lambda_{\mathrm{en}}$, the condition for ions analogous to (C8b) is strongly violated since $T_{\mathrm{i}} \ll T_{\mathrm{e}}$ for an electric field strength up to $2\,\mathrm{V}/\lambda_{\mathrm{en}}$ and we do not require this condition.

For an estimate of Γ_{jsk} with j = i, e, we assume

$$\frac{\mid k \mid e^2}{a_{\mathrm{s}}\,k_B\,T_j} < 1 \quad \text{(C9)}$$

or

$$\mid k \mid < 4 \left(\frac{a_{\mathrm{s}}}{10^{-5}\mathrm{cm}}\right) \left(\frac{T_j}{750\,\mathrm{K}}\right) \quad \text{(C10)}$$

at least for $\mid k \mid \leq 1$. For the electrons conditions (C9) and (C10) are usually fulfilled. For the ions and for $\mid k \mid = 1$ they are usually well fulfilled only for the 1 A.U. standard parameters but may be barely fulfilled for our standard 5 A.U. and dust enriched subdisk parameters due to the low ion temperature there.
For the big grains we proceed from the assumption

$$Z_\mathrm{b}\, e^2/(a_\mathrm{b}\, k_B\, T_j) \gg 1 \tag{C11}$$

or

$$Z_\mathrm{b} \gg 4.5 \times 10^4 \left(\frac{a_\mathrm{b}}{10^{-1}\mathrm{cm}}\right)\left(\frac{T_j}{750\,\mathrm{K}}\right) \tag{C12}$$

We find from our numerical results that condition (C12) is well fulfilled for our standard parameters, at least for distances $z \geq 10^7$ cm.
We assume that

$$\Gamma_{jsk} \approx \Gamma_{js0} \tag{C13}$$

$$\Gamma_\mathrm{ib}\, n_\mathrm{b} \ll \sum_k \Gamma_{\mathrm{is}k}\, n_{\mathrm{s}k} \approx \Gamma_\mathrm{is0}\, n_\mathrm{s} \tag{C14}$$

which is consistent with assumption (C9) and $Z_\mathrm{b} > 0$ and with our standard parameters. For local equilibrium, (1) and (C14) yield (A9), and (2b) and (C13) yield (A10).

We now consider the conditions under which we can neglect the terms $(E/(2\pi e))\,(4\pi a_\mathrm{b}^2)/\tau_\mathrm{bs}$ and $\sum_k k\, n_{sk}(v_{sk} - v_\mathrm{b})\,\pi a_\mathrm{b}^2$ in (A13) compared to $\Gamma_\mathrm{eb}\, n_\mathrm{e}$.

From (A10) and evaluating Γ_eb and Γ_es0 with (C8a) through (C12) we get

$$\Gamma_\mathrm{eb}\, n_\mathrm{e} \approx \left(\frac{-Z_\mathrm{b}/\hat{Z}_\mathrm{b}}{1 + Z_\mathrm{b}/\hat{Z}_\mathrm{b}}\right)\frac{\zeta\, n_\mathrm{n}}{n_\mathrm{b}} \tag{C15}$$

with

$$Z_\mathrm{b}/\hat{Z}_\mathrm{b} \approx \frac{\Gamma_\mathrm{eb}\, n_\mathrm{b}}{\Gamma_\mathrm{es0}\, n_\mathrm{s}} \tag{C16}$$

and

$$\hat{Z}_\mathrm{b} \equiv \frac{a_\mathrm{b}\, k_B T_\mathrm{e}\, \pi a_\mathrm{s}^2\, n_\mathrm{s}}{\pi a_\mathrm{b}^2\, e^2\, n_\mathrm{b}} = 4.5 \times 10^8 \left(\frac{T_\mathrm{e}}{750\,\mathrm{K}}\right)\left(\frac{\rho_\mathrm{s}/\rho_\mathrm{n}}{5\times 10^{-3}}\right) \times \left(\frac{a_\mathrm{b}}{10^{-1}\mathrm{cm}}\right)^2 \left(\frac{\rho_\mathrm{sp,b}}{1\,\mathrm{g\,cm^{-3}}}\right) \times \left(\frac{a_\mathrm{s}}{10^{-5}\mathrm{cm}}\right)^{-1} \left(\frac{\rho_\mathrm{sp,s}}{1\,\mathrm{g\,cm^{-3}}}\right)^{-1} \left(\frac{\rho_\mathrm{b}/\rho_\mathrm{n}}{5\times 10^{-3}}\right)^{-1} \tag{C17}$$

According to our calculations of the electron temperature, T_e increases with E from $T_\mathrm{e} = T_\mathrm{n}$ at $E = 0$ up to $T_\mathrm{e} = 10^4$ K at $E \geq 0.2\,\mathrm{Volts}/\lambda_\mathrm{en}$, implying with (C17) a variation of $\hat{Z}_\mathrm{b}$ with E. For local equilibrium we have $T_\mathrm{e} = 3.9 \times 10^3$ K for our standard 1 A.U. parameters, $T_\mathrm{e} = 7.5 \times 10^2$ K for our standard 5 A.U. parameters, and $T_\mathrm{e} = 3.4 \times 10^3$ K for our standard parameters for the dust enriched subdisk so that we find from (C17) $\hat{Z}_\mathrm{b} = 2.3\times 10^9$; 4.5×10^8; and 5.1×10^8 for our standard 1 A.U., 5 A.U., and dust enriched subdisk parameters, respectively. Taking $Z_\mathrm{b} = 4 \times 10^8$ as derived from approximation (A15), we find that the factor $(Z_\mathrm{b}/\hat{Z}_\mathrm{b})\,(1 + Z_\mathrm{b}/\hat{Z}_\mathrm{b})^{-1}$ in (C15) is 0.15; 0.47; and 0.44, respectively.

Requiring

$$\left(\frac{3\,E}{4\pi e}\right)\left(\frac{4\pi a_\mathrm{b}^2}{\tau_\mathrm{bs}}\right) \ll \mid \Gamma_\mathrm{eb}\, n_\mathrm{e} \mid \tag{C18}$$

we get with (C1), (C4), (C5), definition (A14) and approximation (C15) that

$$E \ll 0.7 \times 10^3\,(\mathrm{V}/\lambda_\mathrm{en})\left(\frac{1}{\gamma}\right)\left(\frac{Z_\mathrm{b}/\hat{Z}_\mathrm{b}}{1 + Z_\mathrm{b}/\hat{Z}_\mathrm{b}}\right)\left(\frac{\zeta}{10^{-22}\mathrm{s^{-1}}}\right) \times \left(\frac{a_\mathrm{s}}{10^{-5}\mathrm{cm}}\right)\left(\frac{\rho_\mathrm{sp,s}}{1\,\mathrm{g\,cm^{-3}}}\right)\left(\frac{T_\mathrm{n}}{750\,\mathrm{K}}\right)^{1/2} \times \left(\frac{\rho_\mathrm{s}/\rho_\mathrm{n}}{5\times 10^{-3}}\right)^{-1}\left(\frac{\rho_\mathrm{b}/\rho_\mathrm{n}}{5\times 10^{-3}}\right)^{-1} \times \left(\frac{g}{-5\times 10^{-2}\mathrm{cm\,s^{-2}}}\right)^{-1}\left(\frac{n_\mathrm{n}}{10^{14}\mathrm{cm^{-3}}}\right)^{-1} \tag{C19}$$

Requiring

$$\left|\sum_k k\, n_{sk}\,(v_{sk} - v_\mathrm{b})\,\pi a_\mathrm{b}^2\right| \ll \mid \Gamma_\mathrm{eb}\, n_\mathrm{e}\mid \tag{C20}$$

we get with (C1) through (C7) and with (C15) that

$$\left|\sum_k \frac{k\, n_{sk}}{n_\mathrm{s}}\right| \ll 3.8 \times 10^{-2}\left(\frac{Z_\mathrm{b}/\hat{Z}_\mathrm{b}}{1 + Z_\mathrm{b}/\hat{Z}_\mathrm{b}}\right) \times \left(\frac{\zeta}{10^{-22}\mathrm{s^{-1}}}\right)\left(\frac{a_\mathrm{s}}{10^{-5}\mathrm{cm}}\right)^3\left(\frac{\rho_\mathrm{sp,s}}{1\,\mathrm{g\,cm^{-3}}}\right)\left(\frac{T_\mathrm{n}}{750\,\mathrm{K}}\right)^{1/2} \times \left(\frac{\rho_\mathrm{s}/\rho_\mathrm{n}}{5\times 10^{-3}}\right)^{-1}\left(\frac{\rho_\mathrm{b}/\rho_\mathrm{n}}{5\times 10^{-3}}\right)^{-1}\left(\frac{g}{-5\times 10^{-2}\mathrm{cm\,s^{-2}}}\right)^{-1} \tag{C21}$$

In addition, in (A13) we can neglect $\Gamma_\mathrm{ib}\, n_\mathrm{i}$ compared to $\Gamma_\mathrm{eb}\, n_\mathrm{e}$ if

$$\Gamma_\mathrm{ib}\, n_\mathrm{i} \ll \mid \Gamma_\mathrm{eb}\, n_\mathrm{e} \mid \tag{C22}$$

With (A9) we get that

$$\Gamma_\mathrm{ib}\, n_\mathrm{i} \approx \frac{\zeta\, n_\mathrm{n}}{n_\mathrm{s}}\frac{\Gamma_\mathrm{ib}}{\Gamma_\mathrm{is0}} \tag{C23}$$

With (C11) and (C23) we estimate that

$$\Gamma_\mathrm{ib}\, n_\mathrm{i} \ll \frac{\zeta\, n_\mathrm{n}}{n_\mathrm{s}}\frac{a_\mathrm{b}^2}{a_\mathrm{s}^2} \tag{C24}$$

If

$$\frac{\zeta\, n_\mathrm{n}}{n_\mathrm{s}}\frac{a_\mathrm{b}^2}{a_\mathrm{s}^2} \ll \mid \Gamma_\mathrm{eb}\, n_\mathrm{e} \mid \tag{C25}$$

which with (C15) is equivalent with

$$\frac{Z_\mathrm{b}/\hat{Z}_\mathrm{b}}{1+Z_\mathrm{b}/\hat{Z}_\mathrm{b}} \gg 10^{-4} \left(\frac{a_\mathrm{s}}{10^{-5}\mathrm{cm}}\right) \left(\frac{\rho_\mathrm{sp,s}}{1\,\mathrm{g\,cm^{-3}}}\right) \left(\frac{\rho_\mathrm{b}/\rho_\mathrm{n}}{5\times10^{-3}}\right) \times \left(\frac{\rho_\mathrm{s}/\rho_\mathrm{n}}{5\times10^{-3}}\right)^{-1} \left(\frac{a_\mathrm{b}}{10^{-1}\mathrm{cm}}\right)^{-1} \left(\frac{\rho_\mathrm{sp,b}}{1\,\mathrm{g\,cm^{-3}}}\right)^{-1} \tag{C26}$$

then condition (C22) is fulfilled. From (C17) and $T_\mathrm{e} \leq 10^4\,\mathrm{K}$ we see that for parameters with values near the standard ones (C26) is fulfilled if Z_b can be approximated by (A15) which is justified below.

In order to arrive at approximation (A15) we neglect the term $\Gamma_\mathrm{eb}\, n_\mathrm{e}$ in (A13), requiring that

$$\mid \Gamma_\mathrm{eb} n_\mathrm{e} \mid \ll \left| \left(\frac{\delta Q_\mathrm{s}\, a_\mathrm{s}}{e}\right) \left(\frac{4\pi a_\mathrm{b}^2}{\gamma\pi a_\mathrm{s}^2}\right) \frac{1}{\tau_\mathrm{bs}} \right| \tag{C27}$$

Using definition (A14), approximation (C15) and assumptions (C1) through (C7) we get from (C27) that

$$\frac{Z_\mathrm{b}/\hat{Z}_\mathrm{b}}{1+Z_\mathrm{b}/\hat{Z}_\mathrm{b}} \left(\frac{\zeta}{10^{-22}\mathrm{s^{-1}}}\right) \left(\frac{a_\mathrm{s}}{10^{-5}\mathrm{cm}}\right)^2 \left(\frac{\rho_\mathrm{sp,s}}{1\,\mathrm{g\,cm^{-3}}}\right) \times \left(\frac{T_\mathrm{n}}{750\,\mathrm{K}}\right)^{1/2} \left(\frac{\delta Q_\mathrm{s}}{-1.44\times10^{-2}\mathrm{V}}\right)^{-1} \left(\frac{\rho_\mathrm{s}/\rho_\mathrm{n}}{5\times10^{-3}}\right)^{-1} \times \left(\frac{\rho_\mathrm{b}/\rho_\mathrm{n}}{5\times10^{-3}}\right)^{-1} \left(\frac{g}{-5\times10^{-2}\mathrm{cm\,s^{-2}}}\right)^{-1} \ll 27 \tag{C28}$$

From our numerical results we find that conditions (C19), (C21) and (C26) are fairly well fulfilled for our standard parameters, at least for distances $z \geq 10^7$ cm. The left hand sides are usually lower than the corresponding right hand sides by an order of magnitude or more, except for (C19) in the case of the standard 1 A.U. parameters (corresponding to the upper curve in Fig. 1) where E is lower than the right hand side of (C19) only by a factor 3 near the peak of the electric field and except for (C21) in the case of the standard parameters for the dust enriched subdisk (corresponding to Fig. 6) where the left hand side is lower than the right hand side only by a factor less than 2 for a large distance range. Condition (C28) is well fulfilled for our standard 1 A.U. and dust enriched subdisk parameters. For our standard 5 A.U. parameters it is also well fulfilled for distances up to 10^{13} cm and somewhat beyond where the medium has not yet reached charge equilibrium but is only barely fulfilled for local equilibrium.

In order to find approximation (A17) we consider an estimate for the frequencies $\nu_{k'k}$. From (A13), (C18), (C20), and (C22) we get for local equilibrium that

$$Z_\mathrm{b} \approx -\left(\frac{\delta Q_\mathrm{s}\, a_\mathrm{s}}{e}\right) \left(\frac{4\pi a_\mathrm{b}^2}{\gamma\pi a_\mathrm{s}^2}\right) + \Gamma_\mathrm{eb}\, n_\mathrm{e}\, \tau_\mathrm{bs} \tag{C29}$$

(C29) gives a somewhat more accurate estimate for Z_b than (A15) where the term $\Gamma_\mathrm{eb}\, n_\mathrm{e}\, \tau_\mathrm{bs}$ decreases Z_b as compared to approximation (A15) due to electron impact on the big grains. In addition, we require that

$$\frac{3}{4\,\pi} \frac{E\,\gamma\pi a_\mathrm{s}^2}{e} \ll \left| \frac{Z_\mathrm{b}\,\gamma\pi a_\mathrm{s}^2}{4\pi a_\mathrm{b}^2} + \frac{\delta Q_\mathrm{s}\, a_\mathrm{s}}{e} \right| \tag{C30}$$

which with (C29) we see is fulfilled if (C18) is fulfilled. Requirement (C30) implies that we can neglect electrostatic polarization of grain material in (16b), (17b), and (18) so that (16a), (16b), and (18) yield with (C30)

$$q_\mathrm{s} = q_\mathrm{sl} + e \approx q_\mathrm{su} - e \tag{C31}$$

From (C31), (16a), (C29), (C15), (A14), and (C1) through (C7),

$$\frac{q_\mathrm{s}}{e} = \frac{q_\mathrm{sl}}{e} + 1 \approx \frac{q_\mathrm{su}}{e} - 1 \approx -3.8\times10^{-2} \left(\frac{Z_\mathrm{b}/\hat{Z}_\mathrm{b}}{1+Z_\mathrm{b}/\hat{Z}_\mathrm{b}}\right) \times \left(\frac{\zeta}{10^{-22}\mathrm{s^{-1}}}\right) \left(\frac{a_\mathrm{s}}{10^{-5}\mathrm{cm}}\right)^3 \left(\frac{\rho_\mathrm{sp,s}}{1\,\mathrm{g\,cm^{-3}}}\right) \left(\frac{T_\mathrm{n}}{750\,\mathrm{K}}\right)^{1/2} \times \left(\frac{\rho_\mathrm{s}/\rho_\mathrm{n}}{5\times10^{-3}}\right)^{-1} \left(\frac{\rho_\mathrm{b}/\rho_\mathrm{n}}{5\times10^{-3}}\right)^{-1} \times \left(\frac{g}{-5\times10^{-2}\mathrm{cm\,s^{-2}}}\right)^{-1} \tag{C32}$$

That is, for parameters near the standard ones and for local equilibrium the average charge carried away by a small grain in a collision with a big grain is negative and its magnitude is small compared to one elementary charge.

We require now

$$\frac{2\zeta n_\mathrm{n}}{n_\mathrm{s}} \ll n_\mathrm{b}\,(v_\mathrm{n} - v_\mathrm{b})\,\pi a_\mathrm{b}^2 \tag{C33}$$

which yields together with (C1) through (C4) that

$$\left(\frac{\zeta}{10^{-22}\mathrm{s^{-1}}}\right) \left(\frac{a_\mathrm{s}}{10^{-5}\mathrm{cm}}\right)^3 \left(\frac{\rho_\mathrm{sp,s}}{1\,\mathrm{g\,cm^{-3}}}\right) \left(\frac{T_\mathrm{n}}{750\,\mathrm{K}}\right)^{1/2} \times \left(\frac{\rho_\mathrm{s}/\rho_\mathrm{n}}{5\times10^{-3}}\right)^{-1} \left(\frac{\rho_\mathrm{b}/\rho_\mathrm{n}}{5\times10^{-3}}\right)^{-1} \left(\frac{g}{-5\times10^{-2}\mathrm{cm\,s^{-2}}}\right)^{-1} \ll 13 \tag{C34}$$

Condition (C34), which is well fulfilled for our standard 1 A.U. and dust enriched subdisk parameters and barely fulfilled for our standard 5 A.U. parameters, implies with (C32) that

$$-1 \ll \frac{q_\mathrm{su}}{e} - 1 < 0 \tag{C35}$$

Although (C34) is only barely fulfilled for our standard 5 A.U. parameters condition (C35) holds also in this case.

From (C31), (C35) and definitions of k_l, k_u given in Sect. 3 we get $k_\mathrm{l} = -1$, $k_\mathrm{u} = 0$, and with (17a) and (17c) $\Theta_{k\mathrm{l}} = \pi$, $\Theta_{k\mathrm{u}} = \pi/2$. Then, we get from (19b) immediately that for $k \neq 0$ or $k \neq -1$

$$\nu_{k'k} = 0 \tag{C36}$$

and from (19a) with (16a), (C29), (C30), (A14), and (C5)

$$\nu_{k'0} = n_\mathrm{b}\,(v_\mathrm{n} - v_\mathrm{b})\,\pi a_\mathrm{b}^2 + \frac{n_\mathrm{b}}{n_\mathrm{s}}\,\Gamma_\mathrm{eb}\,n_\mathrm{e} \tag{C37}$$

$$\nu_{k'-1} = -\frac{n_\mathrm{b}}{n_\mathrm{s}}\,\Gamma_\mathrm{eb}\,n_\mathrm{e} \tag{C38}$$

From (C37) and (C38) we get that

$$\nu_{k'0} + \nu_{k'-1} = n_\mathrm{b}\,(v_\mathrm{n} - v_\mathrm{b})\,\pi a_\mathrm{b}^2 \tag{C39}$$

Eq. (3) gives for local equilibrium and for $k = +1$ or $k = -1$ together with (C36), (C38) and (C39)

$$\begin{aligned}&-\frac{n_\mathrm{b}}{n_\mathrm{s}}\,\Gamma_\mathrm{eb}\,n_\mathrm{e}\,\delta_{k,-1}\,n_\mathrm{s} - n_\mathrm{b}\,(v_\mathrm{n} - v_\mathrm{b})\,\pi a_\mathrm{b}^2\,n_{\mathrm{s}k}\\ &+\Gamma_{\mathrm{is}(k-1)}\,n_{\mathrm{s}(k-1)}\,n_\mathrm{i} - \Gamma_{\mathrm{es}(k+1)}\,n_{\mathrm{s}(k+1)}\,n_\mathrm{e}\\ &-(\Gamma_{\mathrm{is}k}\,n_\mathrm{i} - \Gamma_{\mathrm{es}k}\,n_\mathrm{e})\,n_{\mathrm{s}k} = 0\end{aligned} \tag{C40}$$

where $\delta_{k,-1}$ is the Kronecker δ and where $n_\mathrm{s} = \sum_k n_{\mathrm{s}k}$. With (A9), (A10), and (C13) we get that

$$\Gamma_{\mathrm{is}k}\,n_\mathrm{i} - \Gamma_{\mathrm{es}k} n_\mathrm{e} \approx \frac{\zeta n_\mathrm{n}}{n_\mathrm{s}}\left[1 + \left(1 + \frac{\Gamma_\mathrm{eb}\,n_\mathrm{b}}{\Gamma_{\mathrm{es}0}\,n_\mathrm{s}}\right)^{-1}\right] < \frac{2\,\zeta n_\mathrm{n}}{n_\mathrm{s}} \tag{C41}$$

implying with (C33)

$$\Gamma_{\mathrm{is}k}\,n_\mathrm{i} - \Gamma_{\mathrm{es}k}\,n_\mathrm{e} \ll n_\mathrm{b}\,(v_\mathrm{n} - v_\mathrm{b})\,\pi a_\mathrm{b}^2 \tag{C42}$$

Finally, we assume that

$$n_{\mathrm{s}k} \ll n_{\mathrm{s}(k-1)} \qquad \text{for} \quad k > 0 \tag{C43}$$

and

$$n_{\mathrm{s}k} \ll n_{\mathrm{s}(k+1)} \qquad \text{for} \quad k < 0 \tag{C44}$$

Inserting (A9), (A10), (C13), (C42) to (C44) into (C40) we get that

$$n_{\mathrm{s}1} \approx n_{\mathrm{s}\,-1} \approx \frac{\zeta\,n_\mathrm{n}}{\pi a_\mathrm{b}^2\,n_\mathrm{b}\,(v_\mathrm{n} - v_\mathrm{b})} \tag{C45}$$

(C43), (C44), and (C45) yield (A17).

Approximation (A19) is based on (A9) and (A10) and neglect of $\Gamma_\mathrm{eb}\,n_\mathrm{b}$ compared to $\Gamma_{\mathrm{es}0}\,n_\mathrm{s}$ which is correct within an order of magnitude for $Z_\mathrm{b} \le \hat{Z}_\mathrm{b}$ according to (C16). (A19) should be valid for a wide range of parameter values within an order of magnitude, at least for electric field strengths E varying from 0.3 to $1\,\mathrm{V}/\lambda_\mathrm{en}$ and $T_\mathrm{e} \approx 10^4$ K where A varies from about 0.8 to 0.3.

Besides the conditions detailed above on which (A19) to (A21) are based, Eq. (B8) is based also on the assumption $\tau_\mathrm{E} \approx \tau_\mathrm{Es}$ which holds only if the following conditions are both fulfilled

$$\tau_\mathrm{Eb} \gg \tau_\mathrm{Es} \tag{C46}$$

$$\tau_{\mathrm{E}0} \gg \tau_\mathrm{Es} \tag{C47}$$

or, with the use of (A19) to (A21),

$$\begin{aligned}&\left(\frac{\zeta}{10^{-22}\mathrm{s}^{-1}}\right)\left(\frac{a_\mathrm{b}}{10^{-1}\mathrm{cm}}\right)\left(\frac{\rho_{\mathrm{sp,b}}}{1\,\mathrm{g\,cm}^{-3}}\right)\left(\frac{T_\mathrm{n}}{750\,\mathrm{K}}\right)^{1/2}\\ &\times\left(\frac{\delta Q_\mathrm{s}}{-1.44\times10^{-2}\mathrm{V}}\right)^{-2}\left(\frac{\rho_\mathrm{b}/\rho_\mathrm{n}}{5\times10^{-3}}\right)^{-2}\\ &\times\left(\frac{g}{-5\times10^{-2}\mathrm{cm\,s}^{-2}}\right)^{-1} \gg \frac{2\times10^{-2}}{\gamma^2}\end{aligned} \tag{C48}$$

and

$$\begin{aligned}&\left(\frac{\rho_\mathrm{s}/\rho_\mathrm{n}}{5\times10^{-3}}\right)\left(\frac{n_n}{10^{14}\,\mathrm{cm}^{-3}}\right)\left(\frac{a_\mathrm{s}}{10^{-5}\mathrm{cm}}\right)^{-3}\\ &\times\left(\frac{\rho_{\mathrm{sp,s}}}{1\,\mathrm{g\,cm}^{-3}}\right)^{-1}\left(\frac{g}{-5\times10^{-2}\mathrm{cm\,s}^{-2}}\right)^{-1}\\ &\times\left(\frac{\rho_\mathrm{b}/\rho_\mathrm{n}}{5\times10^{-3}}\right)^{-1} A^{-1} \gg 2\times10^{-3}\end{aligned} \tag{C49}$$

For example, for local equilibrium and for our standard parameter values except for δQ_s which is varied, condition (C48) is only valid if $|\ \delta Q_\mathrm{s}\ | \ll 0.1$V, $|\ \delta Q_\mathrm{s}\ | \ll 0.34$V, and $|\ \delta Q_\mathrm{s}\ | \ll 0.03$V for the parameter values given in column 1, column 2 and column 3 of Table 1, respectively. For larger values of $|\ \delta Q_\mathrm{s}\ |$, τ_E in (B3) should be approximated by τ_Eb as given by (A20) yielding a local equilibrium electric field strength given by (B7) if "$<$" is replaced by "$\approx$".

Table 2. List of symbols

	General remarks
(a)	The following list contains only symbols and their definitions which appear in numbered formulas of the paper. The number of the formula where each symbol appears for the first time is given behind the definition of the symbol.
(b)	All vectors (i.e. electric field, gravitational field, electric current, fluid velocities) are directed along the z - direction where z is the space coordinate of our one dimensional stationary models. Except when stated otherwise the symbols corresponding to a vector denote its z - component rather than its absolute value.
	Latin symbols
A	parameter describing the dependence of $\tau_{\mathrm{E}0}$ on the electric field and on the electron temperature (A19)
a_b	radius of big grains (13)
a_s	radius of small grains (14a)
e	elementary charge (6)
E	electric field (6)
E_b	electric field at which for charged big grains the electric force balances the gravitational force (B4)
E_Br	breakdown strength of the electric field, i.e. absolute value of the electric field at which lightning is induced (22)
f_m	maximum ratio of the volume heated to melt solid material to the volume where the electric field reachs breakdown strength (22)
g	effective gravitational acceleration (8)
H_m	energy released per molecule in the discharge channel required for melting solid material (22)

Table 2. (continued)

$H_{\rm Max}$	maximum energy released per molecule in the discharge channel during a discharge (24)
J	electric current defined by (20b). (20a)
k	number of elementary chargies carried by a small grain (k = 0; ±1; ±2; ...;) (9)
$k_{\rm l}$	integer defined by $q_{\rm sl}/e \leq k_{\rm l} < q_{\rm sl}/e + 1$ (19a)
$k_{\rm u}$	integer defined by $q_{\rm su}/e - 1 < k_{\rm u} \leq q_{\rm su}/e$ (19a)
k_B	Boltzmann's constant (11)
L	lengthscale of a region in which the electric field is strong enough to induce lightning (24)
$m_{\rm b}$	mass of a big grain (8)
$m_{\rm e}$	electron mass (7)
$m_{\rm i}$	ion mass (6)
$m_{\rm n}$	mass of a neutral molecule (i.e. H_2 molecule) (11)
$m_{\rm s}$	mass of a small grain (9)
$n_{\rm b}$	number density of the big grains (1)
$n_{\rm e}$	number density of the electrons (2a)
$n_{\rm i}$	number density of the ions (1)
$n_{\rm n}$	number density of the neutrals (i.e. of the H_2 molecules) (1)
$n_{{\rm s}k}$	number density of those small grains that each carry k elementary charges (k = 0; ±1; ±2; ...) (1)
$n_{\rm s}$	number density of the small grains, i.e. $n_{\rm s} \equiv \sum_k n_{{\rm s}k}$ (A9)
$q_{\rm s}$	average charge carried away by a small grain in a big grain - small grain collision (as averaged over many collisions at the same angle Θ) (18)
$q_{\rm su}$	defined by (16a)
$q_{\rm sl}$	defined by (16b)
Q	charge density of the medium in units of the elementary charge (A1)
$T_{\rm e}$	temperature of the electron fluid (12a)
$T_{\rm i}$	temperature of the ion fluid (11)
$T_{\rm m}$	melting temperature for solid material (22)
$T_{\rm n}$	temperature of the neutral fluid (11)
$v_{\rm b}$	velocity of the big grain fluid (4)
$v_{\rm e}$	velocity of the electron fluid (2a)
$v_{\rm i}$	velocity of the ion fluid (1)
$v_{\rm n}$	velocity of the neutral fluid, i.e. of the H_2 gas (6)
$v_{{\rm s}k}$	velocity of the small grain subfluid consisting of those small grains that each carry k elementary charges (3)
w	width of a lightning bolt (24)
$Z_{\rm b}$	number of elementary chargies carried by a big grain (5)
$Z_{\rm b,Q}$	number of elementary chargies which would be carried by a big grain in charge equilibrium if charging of big grains would be determined only by noninductive charge transfer and electrostatic relaxation in collisions with neutral small grains (B6)
$\hat{Z}_{\rm b}$	defined by (C16). (C15)

Greek symbols

γ	free parameter describing the big grain - small grain charge transfer due to electrostatic relaxation (14a)
$\Gamma_{\rm ib}$	rate coefficient for ions to transfer an elementary charge to big grains, i.e. $e\,n_{\rm i}\,\Gamma_{\rm ib}$ is the current of ions onto a big grain (1)
$\Gamma_{{\rm is}k}$	rate coefficient for ions to transfer an elementary charge to those small grains that each carry k elementary charges, i.e. $e\,n_{\rm i}\,\Gamma_{{\rm is}k}$ is the current of ions onto a small grain carrying k elementary charges (1)
$\Gamma_{\rm eb}$	rate coefficient for electrons to transfer an elementary charge to big grains, i.e. $e\,n_{\rm e}\,\Gamma_{\rm eb}$ is the current of electrons onto a big grain. Note that $\Gamma_{\rm eb} < 0$. (2a)

Table 2. (continued)

$\Gamma_{{\rm es}k}$	rate coefficient for electrons to transfer an elementary charge to those small grains that each carry k elementary charges i.e. $e\,n_{\rm e}\,\Gamma_{{\rm es}k}$ is the current of electrons onto a small grain carrying k elementary charges. Note that $\Gamma_{{\rm es}k} < 0$. (2a)
$\Gamma_{{\rm s}k{\rm b}}$	rate coefficient for those small grains that each cary k elementary charges to transfer an elementary charge to big grains, i.e. $e\,n_{{\rm s}k}\,\Gamma_{{\rm s}k{\rm b}}$ is the current onto a big grain due to impact of charged small grains carrying k elementary charges (5)
$\delta_{i,j}$	Kronecker symbol (19a)
$\delta q_{\rm b}$	change in the charge of a big grain in a collision with a small grain (14a)
$\delta Q_{\rm s}$	free parameter describing the charge transfer in a big grain - small grain collision due to noninductive charge transfer (14a)
ζ	rate per neutral molecule at which radioactive decays and penetrating cosmic rays induce ionization (1)
Θ	angle between a vector from the center of a big grain to a point on the big grain's surface and the $\hat{z}$ direction (13)
Θ_k	defined by (17a) to (17c)
$\lambda_{\rm en}$	mean free path of the electrons with respect to momentum transfer in collisions with neutral molecules (22)
$\nu_{\rm bn}$	defined such that $m_b\,\nu_{\rm bn}\,(v_{\rm n} - v_{\rm b})$ is the time-averaged frictional force on a big grain due to collisions with neutrals (8)
$\nu_{\rm en}$	defined such that $m_e\,\nu_{\rm en}\,(v_{\rm n} - v_{\rm e})$ is the time-averaged frictional force on an electron due to collisions with neutrals (7)
$\nu_{\rm in}$	defined such that $m_i\,\nu_{\rm in}\,(v_{\rm n} - v_{\rm i})$ is the time-averaged frictional force on an ion due to collisions with neutrals (6)
$\nu_{k'k}$	frequency at which collisions with big grains change the charge on a small grain from k' to k elementary charges (3)
$\nu_{\rm sn}$	defined such that $m_s\,\nu_{\rm sn}\,(v_{\rm n} - v_{{\rm s}k})$ is the time-averaged frictional force on a small grain due to collisions with neutrals (9)
$\rho_{\rm b}$	mass density of the big grain fluid (A18)
$\rho_{\rm n}$	mass density of the neutral gas (A11)
$\rho_{\rm s}$	mass density of the small grain fluid (A11)
$\rho_{\rm sp,b}$	specific mass density inside the big grains (A16)
$\rho_{\rm sp,s}$	specific mass density inside the small grains (A11)
σ	surface charge density on a big grain (13)
$\sigma_{\rm en}$	cross section of neutral molecules for momentum transfer of electrons colliding with the neutral molecules (12a)
$\tau_{\rm bs}$	timescale to reach charge equilibrium for the big grains if this charge equilibrium is dominated by noninductive charge transfer in big grain - small grain collisions (A13)
$\tau_{\rm Br}$	timescale to build the electric field up to breakdown strength $E_{\rm Br}$ (23)
$\tau_{\rm e}$	timescale for the electron number density $n_{\rm e}$ to reach local steady state equilibrium (A12)
$\tau_{\rm E}$	e - folding growth timescale of the electric field (A3)
$\tau_{\rm E0}$	e - folding growth timescale of the electric field if gas phase ions and electrons would be the only charged particles (A5)
$\tau_{\rm Eb}$	e - folding growth timescale of the electric field if charged big grains would be the only charged particles (A6)
$\tau_{\rm Es}$	e - folding growth timescale of the electric field if charged small grains would be the only charged particles (A7)
$\tau_{\rm i}$	timescale for the ion number density $n_{\rm i}$ to reach local steady state equilibrium (A11)
$\tau_{\rm PSN}$	lifetime of the protosolar nebula (23)
$\tau_{\rm sb}$	approximate collision time for the small grains to collide with big grains (A18)

References

Cameron A.G.W., 1966, Earth and Planetary Science Letters 1, 93

Draine B.T., 1986, MNRAS 220, 133

Draine B.T., Roberge W.G., Dalgarno A., 1983, ApJ 264, 485

Dubrulle B., Morfill G., Sterzik M., 1995, Icarus 114, 237

Eisenhour D.D., Buseck P.R., 1995, Icarus 117, 197

Fujii N., Miyamoto M., 1983, Constraints on the heating and cooling processes of chondrule formation. In Chondrules and Their Origins (E. A. King, Ed.), pp. 53-60, Lunar and Planetary Science Institute, Houston.

Gibbard S.G., Levy E.H., Morfill G.E., 1997, Icarus, to be submitted.

Grossman J.N., 1988. Formation of chondrules, In Meteorites and the Early Solar System, (J.F. Kerridge and M.S. Mattheus, Eds.), pp. 680-696, University of Arizona Press, Tuscon.

Havnes O., Hartquist T.W., Pilipp W., 1987, The effects of dust on the ionization structures and dynamics in magnetized clouds. In Physical Processes in Interstellar Clouds (G. E. Morfill and M. Scholer, Eds.), pp. 389-412, D. Reidel Publishing Company, Dordrecht.

Hewins R.H., 1983, Dynamic Crystallization experiments as constraints on chondrule genesis. In Chondrules and Their Origins (E. A. King, Ed.), pp. 122-133, Lunar and Planetary Science Institute, Houston.

Hood L.L., Horanyi M., 1991, Icarus 93, 259

Hood L.L., Horanyi M., 1993, Icarus 106, 179

Horanyi M., Morfill G., Goertz C.K., Levy E.H., 1995, Icarus 114, 174

Kieffer S.W., 1975, Sci 189, 333

Latham J., Mason B.J., 1962, Proc. R. Soc. A266, 387

Levy E.H., 1988, Energetics of chondrule formation. In Meteorites and the Early Solar System, (J.F. Kerridge and M.S. Mattheus, Eds.), pp. 697-711, University of Arizona Press, Tuscon.

Levy E.H., Araki S., 1989, Icarus 81, 74

Love, S.G., Keil K., Scott E.R.D., 1995, Icarus 115, 97

Massey H.S.W. 1969. Electronic and Ionic Impact Phenomena, Vol. II. The Clarendon Press, Oxford.

Morfill G.E., Sterzik M., 1990, Planetary disks: Observations and physical processes. In Formation of Stars and Planets and the Evolution of the Solar System (B. Battrick, Ed.), ESA-SP 315, 219-227, European Space Agency, Paris.

Morfill G., Spruit H., Levy E.H., 1993, Physical processes and conditions associated with the formation of protoplanetary disks. In Protostars and Planets III (E. H. Levy and J. I. Lunine, Eds.), pp. 939-978, Univ. of Arizona Press, Tucson.

Pilipp W., Hartquist T.W., 1994, MNRAS 267, 801

Pilipp W., Hartquist T.W., Morfill G.E., 1992, ApJ 387, 364

Ruzmaikina T.V., Ip W.H., 1994, Icarus 112, 430

Scott E.R.D., Barber D.J., Alexander C.M., Hutchison R., Peck J.A., 1988, Primitive material surviving in chondrites: Matrix. In Meteorites and the Early Solar System, (J.F. Kerridge and M.S. Mattheus, Eds.), pp. 718-745, University of Arizona Press, Tuscon.

Shu F.H., Shang H., Lee T., 1996, Sci 271, 1545

Sonett C.P, 1979, Geophys. Res. Lett. 6, 677

Umebayashi T., Nakano T., 1990, MNRAS 243, 103

Wasson J.T, 1972, Rev. Geophys. Space Phys. 10, 711

Weidenschilling S.J., Cuzzi J.N., 1993, Formation of planetesimals in the solar nebula. In Protostars and Planets III (E. H. Levy and J. I. Lunine, Eds.), pp. 1031-1060, Univ. of Arizona Press, Tucson. 70, 11

Whipple F.L., 1966, Sci 153, 54

Wood J.A., 1984, Earth Planet. Sci. Lett. 70, 11

Wood J.A., 1986, Lunar Planet. Sci. 17, 956